A high-resolution spatial assessment of the impacts of drought variability on vegetation activity in Spain from 1981 to 2015

Sergio M. Vicente-Serrano [1,*], Cesar Azorin-Molina [2], Marina Peña-Gallardo[1], Miquel Tomas-Burguera[3], Fernando Domínguez-Castro [1], Natalia Martín-Hernández[1], Santiago Beguería[3], Ahmed El Kenawy[4], Iván Noguera[1], Mónica García[5]

Family names (or surnames) are underlined

[1]Instituto Pirenaico de Ecología, Spanish National Research Council (IPE-CSIC), Campus de Aula Dei, P.O. Box 13034, E-50059 Zaragoza, Spain; [2]Regional Climate Group, Department of Earth Sciences, University of Gothenburg, Gothenburg, Sweden; [3]Estación Experimental de Aula Dei, Spanish National Research Council (EEAD-CSIC), Zaragoza, Spain; [4]Department of Geography, Mansoura University, 35516, Mansoura, Egypt; [5]Department of Environmental Engineering, Technical University of Denmark, Lyngby, Denmark.

* Corresponding author: Sergio M. Vicente-Serrano (e-mail: svicen@ipe.csic.es)

Abstract: Drought is a major driver of vegetation activity in Spain, with significant impacts on crop yield, forest growth, and the occurrence of forest fires. Nonetheless, the sensitivity of vegetation to drought conditions differs largely amongst vegetation types and climates. We used a high-resolution (1.1 km) spatial dataset of the Normalized Difference Vegetation Index (NDVI) for the whole Spain spanning the period from 1981 to 2015, combined with a dataset of the Standardized Precipitation Evapotranspiration Index (SPEI) to assess the sensitivity of vegetation types to drought across Spain. In specific, this study explores the drought time scales at which vegetation activity shows its highest response to drought severity at different moments of the year. Results demonstrate that –over large areas of Spain– vegetation activity is controlled largely by the interannual variability of drought. More than 90% of the land areas exhibited statistically significant positive correlations between the NDVI and the SPEI during dry summers (JJA). Nevertheless, there are some considerable spatio-temporal variations, which can be linked to differences in land cover and aridity conditions. In comparison to other climatic regions across Spain, results indicate that vegetation types

located in arid regions showed the strongest response to drought. Importantly, this study stresses that the time scale at which drought is assessed is a dominant factor in understanding the different responses of vegetation activity to drought.

Key-words: Drought, NDVI, Vegetation activity, Climatic change, Spain.

1. Introduction

Drought is one of the major hydroclimatic hazards impacting land surface fluxes (Baldocchi et al., 2004; Fischer et al., 2007; Hirschi et al., 2011), vegetation respiration (Ciais et al., 2005), net primary production (Reichstein et al., 2007; Zhao and Running, 2010), primary and secondary forest growth (Allen et al., 2015), and crop yield (Lobell et al., 2015; Asseng et al., 2015). Recently, numerous studies suggested an accelerated impact of drought on vegetation activity and forest mortality under different environmental conditions (Allen et al., 2010, 2015; Breshears et al., 2005) with a reduction in vegetation activity and higher rates of tree decay (e.g. Carnicer et al., 2011; Restaino et al., 2016). Nevertheless, a comprehensive assessment of the impacts of drought on vegetation activity is a challenging task. This is particularly because data on forest conditions and growth are partial, spatially sparse, and restricted to a small number of sampled forests (Grissino-Mayer and Fritts, 1997). Furthermore, the temporal resolution of forest data is insufficient to provide deep insights into the impacts of drought on vegetation activity [e.g. the official forest inventories (Jenkins et al., 2003)]. In addition to these challenges, the spatial and temporal data on crops are often limited, as they are mostly aggregated to administrative levels and provided at the annual scale, with minor information on vegetation activity across the different periods of the year (FAO, 2018). To handle these limitations, numerous studies have alternatively employed the available remotely sensed data to assess the impacts of

drought on vegetation activity (e.g. Ji and Peters, 2003; Wan et al., 2004; Rhee et al., 2010; Zhao et al., 2017).

Several space-based products allow for quantifying vegetation conditions, given that active vegetation respond dissimilarly to the electromagnetic radiation received in the visible and near-infrared parts of the vegetation spectrum (Knipling, 1970). As such, with the available spectral information recorded by sensors on board of satellite platforms, it is possible to calculate vegetation indices and accordingly assess vegetation activity (Tucker, 1979). In this context, several studies have already employed vegetation indices not only to develop drought-related metrics (e.g. Kogan, 1997; Mu et al., 2013), but to determine the impacts of drought on vegetation conditions as well (García et al., 2010; Vicente-Serrano et al., 2013; Zhang et al., 2017). An inspection of these studies reveals that drought impacts can be characterized using vegetation indices, albeit with a different response of vegetation dynamics as a function of a wide-range of factors, including –among others– vegetation type, bioclimatic conditions, and drought severity (Bhuiyan et al., 2006; Vicente-Serrano, 2007; Quiring and Ganesh, 2010; Ivits et al., 2014).

Given high interannual variability of precipitation, combined with the prevailing semi-arid conditions across vast areas of the territory, Spain has suffered from frequent, intense and severe drought episodes during the past decades (Vicente-Serrano, 2006). Nonetheless, in the era of temperature rise, the observed increase in atmospheric evaporative demand (AED) during the last decades has accelerated the severity of droughts (Vicente-Serrano et al., 2014c), in comparison to the severity caused only by precipitation deficits (Vicente-Serrano et al., 2014a; González-Hidalgo et al., 2018). Over Spain, the hydrological and socioeconomic impacts of droughts are well-documented. Hydrologically, droughts are often associated with a decrease in

streamflow and reservoir storages (Lorenzo-Lacruz et al., 2010; Lorenzo-Lacruz et al., 2013). The impacts of drought can extend further to crops, leading to crop failure due to deficit in irrigation water (Iglesias et al., 2003), and even in arable non-irrigated lands (Austin et al., 1998; Páscoa et al., 2017). Over Spain, numerous investigations also highlighted the adverse impacts of drought on forest growth (e.g. Camarero et al., 2015; Gazol et al., 2018; Peña-Gallardo et al., 2018) and forest fires (Hill et al., 2008; Lasanta et al., 2017; Pausas, 2004; Pausas and Fernández-Muñoz, 2012).

Albeit with these adverse drought-driven impacts, there is a lack of comprehensive studies that assess the impacts of drought on vegetation activity over the entire Spanish territory, with a satisfactorily temporal coverage. While numerous studies employed remotely sensed imagery and vegetation indices to analyze spatial and temporal variability and trends in vegetation activity over Spain (e.g. del Barrio et al., 2010; Julien et al., 2011; Stellmes et al., 2013), few attempts have been made to link the temporal dynamics of satellite-derived vegetation activity with climate variability and drought evolution (e.g. Vicente-Serrano et al., 2006; Udelhoven et al., 2009; Gouveia et al., 2012; Mühlbauer et al., 2016). An example is González-Alonso and Casanova (1997) who analyzed the spatial distribution of droughts in 1994 and 1995 over Spain, concluding that the most affected areas are semiarid regions. In their comparison of the MODIS Normalized Difference Vegetation Index (NDVI) data and the Standardized Precipitation Index (SPI) over Spain, García-Haro et al. (2014) indicated that the response of vegetation dynamics to climate variability is highly variable, according to the regional climate conditions, vegetation community, and growth stages. A similar finding was also confirmed by Vicente-Serrano (2007) and Contreras and Hunink (2015) in their assessment of the response of NDVI to drought in semiarid regions of northeast and southeast Spain, respectively. Albeit with these comprehensive efforts, a

107   detailed spatial assessment of the links between droughts and vegetation activity, which

108   covers a long time period (decades), is highly desired for Spain to explore the

109   differences in the response of vegetation activity to drought under different

110   environments with various land cover and vegetation types.

111   The overriding objectives of this study are: i) to determine the possible differences in

112   the response of vegetation activity to drought over Spain, as a function of the different

113   land cover types and climatic conditions; and ii) to explore the drought time scales at

114   which vegetation activity highly responds to drought severity. An innovate aspect of

115   this study is that it provides –for the first time– a comprehensive assessment of the

116   response of vegetation activity to drought using a multidecadal (1981-2015) high spatial

117   resolution (1.1 km) NDVI dataset over the study region.

118

119   **2. Data and methods**

120   *2.1. Datasets*

121   *2.1.1. NDVI data*

122   Globally, there are several NDVI datasets, which have been widely used to analyze

123   NDVI variability and trends (e.g. Slayback et al., 2003; Herrmann et al., 2005;

124   Anyamba and Tucker, 2005) and to assess the links between NDVI and climate

125   variability and drought (e.g. Dardel et al., 2014; Vicente-Serrano et al., 2015; Gouveia

126   et al., 2016). Amongst these global datasets, the most widely used are those derived

127   from the Advanced Very High Resolution Radiometer (AVHRR) sensor on board of the

128   NOAA satellites and those retrieved from the Moderate Resolution Imaging

129   Spectroradiometer (MODIS) data. Both products have been widely employed to

130   evaluate the possible influence of drought on vegetation dynamics in different regions

131   worldwide (e.g. Tucker et al., 2005; Gu et al., 2007; Sona et al., 2012; Pinzon and

132 Tucker, 2014; Ma et al., 2015). While the Global Inventory Modeling and Mapping

133 Studies (GIMMS) dataset from NOAA-AVHRR is available at a semi-monthly

134 temporal resolution for the period from 1981 onwards (Tucker et al., 2005; Pinzon and

135 Tucker, 2014), its spatial resolution is quite low (64 km^2), which makes it difficult to

136 capture the high spatial variability of vegetation cover over Spain. On the other hand,

137 the NDVI dataset derived from MODIS dates back only to 2001 (Huete et al., 2002),

138 which is insufficient to give insights into the long-term response of vegetation activity

139 to drought. To overcome these spatial and temporal limitations, our decision was made

140 to employ a recently developed high-resolution spatial NDVI dataset (Sp_1Km_NDVI),

141 which is available at grid interval of 1.1 km, spanning the period from 1981 onwards. In

142 accordance with GIMMS dataset, Sp_1Km_NDVI is available at a semi-monthly

143 temporal resolution. This dataset has already been validated (Vicente-Serrano et al.,

144 2018), showing high performance in comparison to other available NDVI datasets. As

145 such, it can be used -with confidence- to provide a multidecadal assessment of NDVI

146 variability at high-spatial resolution, especially in areas of highly variable vegetation.

147 Herein, it is noteworthy indicating that the data from the Sp_1Km_NDVI dataset was

148 standardized (sNDVI), so that each series has an average equal to zero and a standard

149 deviation equal to one. This procedure is motivated by the strong seasonality and spatial

150 differences of vegetation activity over Spain. Following this procedure, the magnitudes

151 of all NDVI time series are comparable over space and time. To accomplish this task,

152 the data were fitted to a log-logistic distribution, which shows better skill in

153 standardizing environmental variables, in comparison to other statistical distributions

154 (Vicente-Serrano and Beguería, 2016).

155 In order to limit the possible impact of changes in land cover on the dependency

156 between drought and vegetation cover, we assumed that strong changes in NDVI can be

157 seen as an indicator of changes in land cover. As such, those pixels with strong changes

158 in NDVI during the study period were excluded from the analysis. These pixels were

159 defined after an exploratory analysis in which we tested different thresholds. In specific,

160 we excluded those pixels, which exhibited a decrease in the annual NDVI higher than

161 0.05 units or an increase higher than 0.15 units between 1981 and 2015. The spatial

162 distribution of these pixels (not shown here) concurs well with the areas identified in

163 earlier studies over Spain in which it was an abrupt modification of the land cover type

164 (creation of new irrigated lands, urban expansion, deforestation, etc.) (Lasanta and

165 Vicente-Serrano, 2012; Vicente-Serrano et al., 2018). Furthermore, to avoid the possible

166 influence of spatial autocorrelation, which can occur in areas with dominant positive

167 changes in NDVI due to excessive rural exodus and natural revegetation processes (Hill

168 et al., 2008; Vicente-Serrano et al., 2018), we detrended the standardized NDVI series

169 by means of a linear model. We then add the residuals of the linear trend to the average

170 of NDVI magnitude over the study period. A similar approach has been adopted in

171 several environmental studies (Olsen et al., 2013; Xulu et al., 2018; Zhang et al., 2016).

172 Correlations with the drought dataset were based on the sNDVI.

173

174 *2.1.2. Drought dataset*

175 Due to its complicated physiological strategies to cope with water stress, vegetation can

176 show specific and even individual resistance and vulnerability to drought (Chaves et al.,

177 2003; Gazol et al., 2017; Gazol et al., 2018). As such, it is quite difficult to directly

178 assess the impacts of drought on vegetation activity and forest growth. Alternatively,

179 drought indices can be an appropriate tool to make this assessment, particularly with

180 their calculation at multiple time scales. These time scales summarize the accumulated

181 climatic conditions over different periods, which make drought indices closely related

to impact studies. Overall, to calculate drought indices, we employed data for a set of meteorological variables (i.e. precipitation, maximum and minimum air temperature, relative humidity, sunshine duration, and wind speed) from a recently developed gridded climatic dataset (Vicente-Serrano et al., 2017). This gridded dataset was developed using a dense network of quality-controlled and homogenized meteorological records. Data are available for the whole Spanish territory at a spatial resolution of 1.1 km, which is consistent with the resolution of the NDVI dataset (section 2.1.1). Based on this gridded dataset, we computed the atmospheric evaporative demand (AED) and the Standardized Precipitation Evapotranspiration Index (SPEI). We used the reference evapotranspiration (ETo) as the most realibale way of estimating the AED. ETo was calculated using the physically based FAO-56 Penman-Monteith equation (Allen et al., 1998). On the other hand, the SPEI was computed using precipitation and ETO data (Vicente-Serrano et al., 2010). The SPEI is one of the most widely used drought indices and has thus been employed to quantify drought in a number of agricultural (e.g. Peña-Gallardo et al., 2018b), environmental (e.g. Vicente-Serrano et al., 2012; Bachmair et al., 2018), and socioeconomic applications (e.g. Bachmair et al., 2015; Stagge et al., 2015). The SPEI is advantageous compared to the Palmer Drought Severity Index (PDSI), as it is calculated at different time scales. In comparison to the Standardized Precipitation Index (SPI) (McKee et al., 1993), the SPEI does not account only for precipitation, but it also considers the contribution of ETO in drought evolution.

In this work, the SPEI was calculated for the common 1- to 24-month time scales but here given the semi-monthly availability of the data, we calculated the corresponding 1- to 48- semi-monthly time-scales. The preference to use various time scales is motivated by our intention to characterize the response of different hydrological and environmental systems to drought. It is well-recognized that natural systems can show

different responses to the time scales of drought (Vicente-Serrano et al., 2011, 2013). The time scale refers to the period in which antecedent climate conditions are accumulated and it allows adapting the drought index to the drought impacts since different hydrological and environmental systems show different responses sensitivities to the time scales of climate variability. This has been shown for hydrological systems (López-Moreno et al., 2013; Barker et al., 2016), but also ecological and agricultural systems show strong differences in the response to different time scales of climatic droughts (Pasho et al., 2011; Peña-Gallardo et al., 2018b) given different biophysical conditions, but also the different strategies of vegetation types to cope with water stress (Chaves et al., 2003; McDowell et al., 2008), which are strongly variable in complex Mediterranean ecosystems. For instance, drought indices can be calculated on flexible time scales since it is not known a priori the most suitable period at which the NDVI is responding. Herein, we also detrended and standardized the semi-monthly SPEI data to be comparable with the de-trended sNDVI.

Finally, we used the CORINE Land Cover for 2000 (https://land.copernicus.eu/pan-european/corine-land-cover) to determine how land cover can impact the response of NDVI to drought severity. This map is representative of the main classes of land cover in the study domain over the period of investigation.

2.2. Statistical analysis

We used the Pearson's *r* correlation coefficient to assess the relationship between the interannual variability of the sNDVI and SPEI. This association was evaluated independently for each semi-monthly period of the year. In specific, we calculated the correlation between the sNDVI for each semi-monthly period and SPEI recorded in the same period, at time-scales between 1- and 48-semi-months. Significant correlations

232   were set at $p < 0.05$. Importantly, as the data of the sNDVI and SPEI were de-trended,

233   the possible impact of serial correlation on the correlation between sNDVI and SPEI is

234   minimized, with no spurious correlation effects that can be expected from the co-

235   occurrence of the trends. Similarly, as the data were analyzed for each semi-monthly

236   period independently, our results are free from any seasonality effect. Given that it is

237   not possible to know a priori the best cumulative period to explain the response of the

238   vegetation activity to drought variability, we retained for further analysis the maximum

239   correlation, independently of the time scale at which this is obtained.

240   Based on the correlation coefficients between the sNDVI and SPEI in the study domain,

241   we determined the semi-monthly period of the year and the SPEI time scale at which the

242   maximum correlation is found. This information was then used to determine the spatial

243   and seasonal variations according to the different land cover categories. Finally, the

244   average climate conditions over the study domain, including aridity (precipitation minus

245   ETO) and average temperature, were related to the time-scales at which the maximum

246   correlation between the sNDVI and SPEI was found.

247

248   **3. Results**

249   *3.1. General influence of drought on the sNDVI*

250   Figure 1 shows an example of the spatial distribution of the Pearson's r correlation

251   coefficients calculated between the sNDVI and the SPEI at the time-scales of 1-, 3-, 6-

252   and 12-months (2-, 6-, 12- and 24-semi-monthly periods). Results are shown only for

253   the second semi-monthly period of each month between April and July. The differential

254   response of the NDVI to the different time scales of the SPEI is illustrated. As depicted,

255   the 6-month time scale was more relevant to vegetation activity in large areas of

256   Southwestern and Southeastern Spain during the second half of April. On the other

257   hand, vegetation activity was more determined by the 12-month SPEI across the Ebro

258   basin in northeastern Spain. This stresses the need of considering different drought time

259   scales to know the climate cumulative period that mostly affects vegetation activity. The

260   6-month and 12-month SPEI produced similar results during the second period of May,

261   while the 12-month time scale is more related to vegetation activity in June and July.

262   Figure 2 summarizes the maximum correlation between the sNDVI and the SPEI,

263   providing insights into the differential response of the NDVI to drought. It can be noted

264   that there are clear seasonal and spatial differences in the response of sNDVI to the

265   SPEI. The sNDVI is more related to the SPEI during the warm season (MJJA). In

266   contrast, the response of the sNDVI to drought is less pronounced from September to

267   April, albeit with some exceptions. One example is the response of vegetation to

268   drought alongside the southeastern Mediterranean coastland, where the correlation

269   between sNDVI and SPEI is almost high all the year around. Table 1 summarizes the

270   percentage of the total area exhibiting significant or non-significant correlations over

271   Spain during the different semi-monthly periods. Positive (lower sNDVI with drought)

272   and statistically significant correlations are dominant across the entire territory, but with

273   a seasonal component. In particular, a higher percentage of the territory shows positive

274   and significant correlations during the warm season (MJJA). From mid of May to mid

275   of September, more than 80% of the study domain show positive and significant

276   correlations between the sNDVI and the SPEI. A similar finding is also found between

277   the mid of June and the beginning of August. Figure 3 summarizes the average

278   correlations between the SPEI and sNDVI. As illustrated, there is a gradual increase in

279   the response of the sNDVI to the SPEI from the beginning of May to the end of July,

280   when the maximum average correlation is recorded. In contrast, the correlations

281   between the SPEI and sNDVI decrease progressively from August to December.

282   The response of the sNDVI to different times scales of the SPEI and seasons is quite

283   complex. Figure 4 shows the spatial distribution of the SPEI time scale at which the

284   maximum correlation was found for each one of the 24 semi-monthly periods of the

285   year. It can be noted that there are considerable seasonal and spatial differences.

286   Nonetheless, these differences are masked with the estimated average values of the

287   SPEI time scale recorded for the semi-monthly periods (Figure 5) which are less

288   variable (oscillating between 18 and 22 semi-monthly periods -9 to 11 months-)

289   throughout the year. In general, the areas and periods with higher correlations are

290   recorded at the time scales between 7 and 24 semi-months (3-12 months).

291

292   *3.2. Land cover differences*

293   There are differences in the magnitude and seasonality of the Pearson's r correlation

294   coefficients among all land cover types. Figure 6 shows the average and standard error

295   of the mean of the maximum Pearson's r coefficients between the sNDVI and SPEI for

296   the different land cover types and the 24 semi-monthly periods. The magnitudes of

297   correlation vary considerably, as a function of land cover type, as well as the period of

298   the year in which the highest correlations are recorded. The non-irrigated arable lands

299   show a peak of significant correlation between April and June. However, this

300   correlation decreases towards the end of the year. The majority of this land cover shows

301   positive and significant correlations between May and September (Supplementary Table

302   1), with percentages almost close to 100%. On the contrary, irrigated lands do not show

303   such a strong response to drought during the warm season. Even with the presence of a

304   seasonal pattern, it is less pronounced than the one observed for non-irrigated arable

305   lands. Overall, irrigated areas are characterized by positive and significant correlations

306   between sNDVI and SPEI during summertime (Supplementary Table 2). Similarly,

307 vineyards show a clear seasonal pattern, albeit with a peak of maximum correlations

308 during the late summer (July-August) and early autumn (September-October)

309 (Supplementary Table 3). On the other hand, olive groves show of the highest

310 correlation between the sNDVI and SPEI during the second half of May and in October,

311 suggesting a quasi bi-modal response of the NDVI to drought. This pattern is also

312 revealed in the percentage of the surface area with significant correlations

313 (Supplementary Table 4). In the same context, the areas of natural vegetation exhibit

314 their maximum correlation between the sNDVI and SPEI during summer months. The

315 highest correlations are found in July and August for the forest types, compared to

316 earlier June for the natural grasslands and the areas of sclerophillous vegetation. On the

317 other hand, the mixed forests tend to show lower correlations than broad-leaved and

318 coniferous forests. A quick inspection of all these types of land cover indicates that the

319 correlations between the sNDVI and SPEI are generally positive and significant during

320 summer months (Supplementary Tables 5 to 11).

321 Large differences across vegetation types were found for the SPEI time scales at which

322 maximum correlations between sNDVI and the SPEI are found (Figure 7). For example,

323 for non-irrigated arable lands, the maximum correlation between SPEI and sNDVI is

324 found for time scales between 11 and 21 semi-monthly periods. This indicates that

325 crops in May-June (the period in which higher correlations are recorded) respond

326 mostly to the climate conditions recorded between June and December of the preceding

327 year. Irrigated lands show a clear seasonal pattern, as maximum correlations are

328 recorded at time scales between 12 and 18 semi-monthly periods (i.e. 6 to 9 months),

329 mainly between November and May. On the other hand, the maximum correlations

330 between sNDVI and SPEI during summer are found for time scales between 25 and 28

331 semi-monthly periods. Similar to irrigated lands, vineyards show a strong seasonality,

332 responding to longer time-scales at the end of summertime. In contrast, natural

333 vegetation areas show less seasonality to SPEI time scales, which mostly impact the

334 interannual variability of sNDVI. The SPEI time scales, at which the maximum

335 correlation is found between sNDVI and SPEI, vary from 20 semi-monthly periods

336 during the warm season (MJJAS) to 30 semi-monthly periods during the cold season

337 (ONDJFMA). This finding is evident for all forest types and areas of sclerophillous

338 vegetation and mixed wood-scrub. The only exception corresponds to natural

339 grasslands, which show a response to shorter SPEI time scales (i.e. 20 semi-monthly

340 periods in winter and 15 in spring and early summer).

341

342 *3.3. Influence of average climatic conditions*

343 In addition to the impact of the time scale at which drought is quantified, the response

344 of vegetation activity to drought can also be closely related to the prevailing climatic

345 conditions. Figure 8 summarizes the spatial correlation between aridity (P-ETo) and the

346 maximum correlation between the sNDVI and SPEI. For most of the semi-monthly

347 periods of the year aridity is negatively correlated with the maximum correlation

348 between sNDVI and SPEI, indicating that vegetation activity in arid sites is more

349 responsive to drought variability. This correlation is more pronounced for the period

350 between December and June. In contrast, this negative association becomes weaker and

351 statistically non-significant during warmer months (July to August). Figure 9 illustrates

352 the spatial correlation between mean air temperature and the maximum correlation

353 between the sNDVI and SPEI. Results demonstrate similar results to those found for

354 aridity, with a general positive and significant correlation from March to June, followed

355 by a non-significant and weak correlation during summer months.

356   Nonetheless, these general patterns vary largely as a function of land cover type

357   (Supplementary Figures 1 to 11). For example, in non-irrigated arable lands, there is

358   strong negative correlation between aridity and the sNDVI/SPEI maximum correlation

359   from March to May: a period that witnesses the peak of vegetation activity in this land

360   cover type. This also coincides with the period of the highest average correlations

361   between the sNDVI and SPEI. Taken together, this demonstrates that non-irrigated

362   arable lands located in the most arid areas are more sensitive to drought variability than

363   those located in humid regions. As opposed to non-irrigated arable lands, the

364   correlations with aridity are found statistically non-significant in all periods of the year

365   for irrigated lands, vineyards and olive groves. Nevertheless, for the different natural

366   vegetation categories, the correlations are negative and statistically significant during

367   large periods. The mixed agricultural/natural vegetation areas show a significant

368   correlation between October and July, with stronger association at the beginning of

369   summer season. Broadleaved and coniferous forests, scrubs, and pasture lands also

370   show a negative relationship between the spatial patterns of the sNDVI/SPEI

371   correlations and aridity.

372   As depicted in Figure 9, the relationship between the sNDVI/SPEI correlation and air

373   temperature shows that the response of vegetation activity to drought is modulated by

374   air temperature during springtime. This implies that warmer areas are those in which the

375   sNDVI is more controlled by drought. A contradictory pattern is found during warmer

376   months, in which the role of air temperature in modulating the impact of drought on

377   vegetation activity is minimized. The relationships between air temperature and the

378   NDVI-SPEI correlation vary among the different land cover types (Supplementary

379   Figures 12 to 22). For example, in non-irrigated arable lands, the positive and

380   statistically significant correlation is found in the period from March to May, indicating

381   that the response of the sNDVI to SPEI tends to coincide spatially with areas of warmer

382   conditions. As observed for aridity, the relationship between the sNDVI and SPEI in

383   irrigated lands is less associated with the spatial patterns of air temperature. A similar

384   pattern is recorded for vineyards and olive groves. Nevertheless, the areas of natural

385   vegetation show a clear relationship between air temperature and the sNDVI/SPEI

386   correlations. In the mixed agriculture and natural vegetation areas, we found a

387   statistically significant positive association between the sNDVI and SPEI from October

388   to May. On the contrary, this association is less evident during summer months. This

389   general association during springtime, combined with the lack of association during

390   summertime, can also be seen for other natural vegetation types such as broad-leaved

391   and coniferous forests, natural grasslands, sclerophillous vegetation and mixed wood-

392   scrubs.

393   We also analyzed the dependency between climatic conditions (i.e. aridity and air

394   temperature) and the SPEI time scale(s) at which the maximum correlation between the

395   sNDVI and SPEI is recorded. Figure 10 shows the values of aridity corresponding to

396   SPEI time scales at which the maximum correlation between the sNDVI and SPEI is

397   found for each semi-monthly period. The different box-plots indicate complex patterns,

398   which are quite difficult to interpret. Overall, less arid areas show stronger correlations

399   at longer time-scales (25-42 semi-monthly periods) during springtime. In the same

400   context, the regions with maximum correlations at short time scales (1-6 months) tend

401   to be located in less arid regions that record their maximum correlations at time scales

402   between 7 and 24 semi-monthly periods. This suggests that the most arid areas mostly

403   respond to the SPEI time scales between 6 and 12 months, compared to short (1-3

404   months) or long (> 12 months) SPEI time-scales in more humid regions. In contrast,

405   during summer season, the interannual variability of the sNDVI in the arid areas is

mostly determined by the SPEI recorded at time scales higher than 6 months (12 semi-monthly periods), while responding to short SPEI time scales (< 3 months) over the most humid regions.

Also, we found links between the spatial distribution of air temperature and the SPEI time scales at which maximum correlation between the sNDVI and SPEI is recorded (Figure 11). In early spring, short SPEI time scales dominate in warmer areas, compared to long SPEI time scales in colder regions. A contradictory pattern is observed from June to September, with a dominance of shorter SPEI time scales in colder areas and longer SPEI time scales in warmer regions.

The spatial distribution of all land cover types, after excluding irrigated lands in which the anthropogenic factors dominate, is illustrated in Figure 12. Mixed forests are located in the most humid areas, while vineyards, olive groves, non-irrigated arable lands and the sclerophyllous natural vegetation are distributed in the most arid sites. Nevertheless, there is a gradient of these land cover types in terms of their response to drought, as those types located under more arid conditions show a stronger response of vegetation activity to drought than those located in humid environments. For example, the mixed forests show lower correlations than crop types and other vegetation areas. This pattern is more evident during the different semi-monthly periods, albeit with more differences during spring and autumn. In summer, these differences are much smaller between land cover categories, irrespective of aridity conditions.

There are also differences in the average SPEI time scale at which the maximum sNDVI/SPEI correlation is obtained (Figure 13). However, these differences are complex, with noticeable seasonal differences in terms of the relationship between climate aridity and land cover types. In spring and late autumn, land cover types located in more arid conditions tend to respond to shorter SPEI time scales than those located in

431 more humid areas. This pattern can be seen in late summer and early autumn, in which

432 the most arid land cover types (e.g. vineyards and olive groves) tend to respond at

433 longer SPEI time scales, compared to forest types (mostly the mixed forests), which are

434 usually located under more humid conditions.

435

436 **4. Discussion**

437 This study assesses the response of vegetation activity to drought in Spain using a high-

438 resolution (1.1 km) spatial NDVI dataset that dates back to 1981 (Vicente-Serrano et al.,

439 2018). Based on another high-resolution semi-monthly gridded climatic dataset, drought

440 was quantified using the Standardized Precipitation Evapotranspiration Index (SPEI) at

441 different time scales (Vicente-Serrano et al., 2017).

442 Results demonstrate that vegetation activity over large parts of Spain is closely related

443 to the interannual variability of drought. In summer more than 90% of the study domain

444 shows statistically significant positive correlations between the NDVI and SPEI. A

445 similar response of the NDVI to drought is confirmed in earlier studies in different

446 semi-arid and sub-humid regions worldwide, including Northeastern Brazil (e.g.

447 Barbosa et al., 2006), the Sahel (e.g. Herrmann et al., 2005), Central Asia (e.g. Gessner

448 et al., 2013), Australia (e.g. De Keersmaecker et al., 2017) and California (e.g. Okin et

449 al., 2018). Albeit with this generalized response, our results also show noticeable spatial

450 and seasonal differences in this response. These differences can be linked to the time

451 scale at which the drought is quantified, besides the impact of other dominant climatic

452 conditions (e.g. air temperature and aridity).

453

454 *4.1. The response of vegetation activity to drought variability*

455   This study stresses that the response of vegetation activity to drought is more

456   pronounced during the warm season (MJJAS), in which vast areas of the Spanish

457   territory show statistically significant positive correlation between the sNDVI and SPEI.

458   This seasonal pattern can be attributed to the phenology of vegetation under different

459   land cover types. In the cold season, some areas, such as pastures and non-permanent

460   broad leaf forests, do not have any vegetation activity. Other areas, with coniferous

461   forests, shrubs and cereal crops, show a low vegetation activity. As such, irrespective of

462   the recorded drought conditions, the response of vegetation to drought would be low

463   during wintertime. This behaviour is also enhanced by the atmospheric evaporative

464   demand (AED), which is generally low in winter in Spain (Vicente-Serrano et al.,

465   2014d), with a lower water demand of vegetation and accordingly low sensitivity to soil

466   water availability. Austin et al. (1998) indicated that soil water recharge occurs mostly

467   during winter months, given the low water consumption by vegetation. However, in

468   spring, vegetation becomes more sensitive to drought due to temperature rise.

469   Accordingly, the photosynthetic activity, which determines NDVI, is highly controlled

470   by soil water availability (Myneni et al., 1995). In this study, the positive spatial

471   relationship found between air temperature and the sNDVI/SPEI correlation reinforces

472   this explanation. In spring, we found low correlations between the NDVI and SPEI,

473   even in cold areas. In contrast, summer warm temperatures reinforce vegetation activity,

474   but with some exceptions such as cereal cultivations, dry pastures and shrubs. This

475   would explain why the response of vegetation activity to the SPEI is stronger during

476   summer in vast areas of Spain.

477   Also, this study suggests clear seasonal differences in the response of the NDVI to

478   drought, and in the magnitude of the correlation between the NDVI and the SPEI, as a

479   function of the dominant land cover. These differences are confirmed at different spatial

scales, ranging from regional and local (e.g. Ivits et al., 2014; Zhao et al., 2015; Gouveia et al., 2017; Yang et al., 2018) to global (e.g. Vicente-Serrano et al., 2013), Over Spain, the non-irrigated arable lands, natural grasslands and sclerophyllous vegetation show an earlier response to drought, mainly in late spring and early summer. This response is mainly linked to the vegetation phenology dominating in these land covers, which usually reach their maximum activity in late spring to avoid dryness and temperature rise during summer months. The root systems of herbaceous species are not very deep, so they depend on the water storage in the most superficial soil layers (Milich and Weiss, 1997), and they could not survive during the long and dry summer in which the surface soil layers are mostly depleted (Martínez-Fernández and Ceballos, 2003). This would explain an earlier and stronger sensitivity to drought also showed in other world semiarid regions (Liu et al., 2017; Yang et al., 2018; Bailing et al., 2018). On the contrary, maximum correlations between the NDVI and the SPEI are recorded during summer months in the forests but also in wood cultivations like vineyards and olive groves. In this case, the maximum sensitivity to drought coincides with the maximum air temperature and atmospheric evaporative demand (Vicente-Serrano et al., 2014d). This pattern would be indicative of a different adaptation strategy of trees in comparison to herbaceous vegetation, since whilst herbaceous cover would adapt to the summer dryness generating the seed bank before the summer (Peco et al., 1998; Russi et al., 1992), the trees and shrubs would base their adaptation on deeper root systems, translating the drought sensitivity to the period of highest water demand and water limitation.

In addition to the seasonal differences among land cover types, we have shown that in Spain herbaceous crops show a higher correlation between the NDVI and the SPEI than most of natural vegetation types (with the exception of the sclerophyllous vegetation).

505   This behaviour could be explained by three different factors: i) a higher adaptation of

506   natural vegetation to the characteristic climate of the region where drought is a frequent

507   phenomenon (Vicente-Serrano, 2006); ii) the deeper root systems that allow shrubs and

508   trees to obtain water from the deep soil; and iii) cultivated lands tend to be typically

509   located in drier areas than natural vegetation. Different studies showed that the

510   vegetation of dry environments tends to have a more intense response to drought than

511   sub-humid and humid vegetation (Schultz and Halpert, 1995; Abrams et al., 1990;

512   Nicholson et al., 1990; Herrmann et al., 2016). Vicente-Serrano et al. (2013) analysed

513   the sensitivity of the NDVI in the different biomes at a global scale and found a spatial

514   gradient in the sensitivity to drought, which was more important in arid and semiarid

515   regions.

516

517   *4.2. Response to the average climatology*

518   In this study we have shown a control in the response of the NDVI to drought severity

519   by the climatic aridity. Thus, there is a significant correlation between the spatial

520   distribution of the climatic aridity and the sensitivity of the NDVI to drought, mostly in

521   spring and autumn. This could be explained because in more humid environments the

522   main limitation to vegetation growth is temperature and radiation rather than water, so

523   not all the water available would be used by vegetation reflected in a water surplus as

524   surface runoff. This characteristic would make the vegetation less sensitive to drought

525   in the cold season. Drought indices are relative metrics in comparison to the long term

526   climate with the purpose of making drought severity conditions comparable between

527   areas of very different climate characteristics (Mukherjee et al., 2018). This means that

528   in humid areas the corresponding absolute precipitation can be sufficient to cover the

529   vegetation water needs although drought indices inform on below-of-the-average

530 conditions. On the contrary, in arid regions a low value of a drought index is always

531 representative of limited water availability, which would explain the closer relationship

532 between the NDVI and the SPEI.

533 Here we also explored if the general pattern observed in humid and semi-arid regions is

534 also affected by the land cover, and found that the behaviour in the non-irrigated arable

535 lands is the main reason to explain the global pattern. Herbaceous crops show that

536 aridity levels have a clear control of the response of the NDVI to drought during the

537 period of vegetation activity. Nevertheless, after the common harvest period (June) this

538 control by aridity mostly disappears. This is also observed in the grasslands and in the

539 sclerophyllous vegetation, and it could be explained by the low vegetation activity of

540 the herbaceous and shrub species during the summer, given the phenological strategies

541 to cope with water stress with the formation of the seeds before the period of dryness

542 (Chaves et al., 2003). The limiting aridity conditions that characterises the regions in

543 which these vegetation types grow would also contribute to explain this phenomenon.

544 On the contrary, the forests, both broad-leaved and coniferous, also show a control by

545 aridity in the relationship between the NDVI and the SPEI during the summer months

546 since these land cover types show the peak of the vegetation activity during this season.

547 In any case, it is also remarkable that the spatial pattern of the NDVI sensitivity to

548 drought in forests is less controlled by aridity during the summer season, curiously the

549 season in which there are more limiting conditions. This could be explained by the

550 NDVI saturation under high levels of leaf area index (Carlson and Ripley, 1997), since

551 once the tree tops are completely foliated the electromagnetic signal is not sensitive to

552 additional leaf growth. This could explain the less sensitive response of the forests to

553 drought in comparison to land cover types characterised by lower leaf area (e.g. shrubs

554 or grasslands). Nevertheless, we do not think that this phenomenon can explain totally

the decreased sensitivity to drought with aridity in summer since the dominant

coniferous and broad-leaved forests in Spain are usually not characterised by a 100%

leaf coverage (Castro-Díez et al., 1997; Molina and del Campo, 2012), so large signal

saturation problems are not expected. On the other hand, the ecophysiological strategies

of forests to cope with drought may help explain the observed lower relationship

between aridity during the summer months. Experimental studies suggested that the

interannual variability of the secondary growth could be more sensitive to drought than

the sensitivity observed by the photosyntetic activity and the leaf area (Newberry,

2010). This could be a strategy to optimize the storage of carbohydrates, suggesting that

forests in dry years would prioritize the development of an adequate foliar area in

relation to the wood formation in order to maintain respiration and photosynthetic

processes. Recent studies by Gazol et al. (2018) and Peña-Gallardo et al. (2018b)

confirmed that, irrespective of forest species, there is a higher sensitivity of tree-ring

growth to drought, as compared to the sensitivity of the NDVI. The different spatial and

seasonal responses of vegetation activity to drought in our study domain can also be

linked to the dominant forest species and species richness, which has been evident in

numerous studies (e.g. Lloret et al., 2007). Moreover, this might also be attributed to the

ecosystem physiological processes, given that vegetation tends to maintain the same

water use efficiency under water stress conditions, regardless of vegetation types and

environmental conditions (Huxman et al., 2004). This would explain that -

independently of the aridity conditions- the response of the NDVI to drought would be

similar. Here, we demonstrated that the response of the NDVI to drought is similar

during summer months, even with the different land cover types and environmental

conditions.

4.3. The importance of drought time scales

A relevant finding of this study is that the response of the NDVI is highly dependent on the time scale at which drought is quantified. Numerous studies indicated that the accumulation of precipitation deficits during different time periods is essential to determine the influence of drought on the NDVI (e.g. Malo and Nicholson, 1990; Liu and Kogan, 1996; Lotsch et al., 2003; Ji and Peters, 2003; Wang et al., 2003). This is simply because soil moisture is impacted largely by precipitation and the atmospheric evaporative demand over previous cumulative periods (Scaini et al., 2015). Moreover, the different morphological, physiological and phenological strategies would also explain the varying response of vegetation types to different drought time scales. This finding is confirmed in previous works using NDVI and different time scales of a drought index (e.g. Ji and Peters, 2003; Vicente-Serrano, 2007), but also using other variables like tree-ring growth (e.g. Pasho et al., 2011; Arzac et al., 2016; Vicente-Serrano et al., 2014a). This study confirms this finding, given that there is a high spatial diversity in the SPEI time scale at which vegetation has its maximum correlation with the NDVI. These spatial variations, combined with strong seasonal differences, are mainly controlled by the dominant land cover types and aridity conditions. In their global assessment, Vicente-Serrano et al. (2013) found gradients in the response of the world biomes to drought, which are driven mainly by the time scale at which the biome responds to drought in a gradient of aridity. Again, the response to these different time scales implies not only different vulnerabilities of vegetation to water deficits, but also various strategies from plants to cope with drought. In Spain, we showed that the NDVI responds mostly to the SPEI at time scales around 20 semi-monthly periods (10 months), but with some few seasonal differences (i.e. shorter time scales in spring and early autumn than in late summer and autumn). Herein, it is also noteworthy indicating

605   that there are differences in this response, as a function of land cover types. Overall,

606   during the periods of highest vegetation activity, the herbaceous land covers (e.g. non-

607   irrigated arable lands and grasslands) respond to shorter SPEI time-scales than other

608   forest types. This pattern can be seen in the context that herbaceous covers are more

609   dependent on the weather conditions recorded during short periods. These vegetation

610   types could not reach deep soil levels, which are driven by climatic conditions during

611   longer periods (Changnon and Easterling, 1989; Berg et al., 2017). In contrast, the tree

612   root systems would access to these deeper levels, having the capacity of buffering the

613   effect of short term droughts, albeit with more vulnerability to long droughts that

614   ultimately would affect deep soil moisture levels. This pattern has been recently

615   observed in southeastern Spain when comparing herbaceous crops and vineyards

616   (Contreras and Hunink, 2015). Recently, Okin et al. (2018) linked the different

617   responses to drought time scales between scrubs and chaparral herbaceous vegetation in

618   California to soil water depletion at different levels.

619   Albeit with these general patterns, we also found some relevant seasonal patterns. For

620   example, irrigated lands responded to long SPEI time scales (> 15 months) during

621   summer months, whilst they responded to shorter time scales (<7 months) during spring

622   and autumn. This behaviour can be linked to water management in these areas. In

623   specific, during spring months, these areas do not receive irrigation and accordingly

624   vegetation activity is determined by water stored in the soil. On the contrary, summer

625   irrigation depends on the water stored in the dense net of reservoirs existing in Spain;

626   some of them have a multiannual capacity. Water availability in the reservoirs usually

627   depends on the climate conditions recorded during long periods (one or two years)

628   (López-Moreno et al., 2004; Lorenzo-Lacruz et al., 2010), which determine water

629   availability for irrigation. This explains why vegetation activity in irrigated lands

630   depends on long time scales of drought. Similarly, vineyards and olive groves respond

631   to long SPEI time-scales during summer. These cultivations are highly resistant to

632   drought stress (Quiroga and Iglesias, 2009). However, these adapted cultivations can be

633   sensitive to severe droughts under extreme summer dryness. In comparison to other

634   natural vegetation, mixed forests show response to shorter SPEI time scales. This could

635   be explained by the low resistance of these forest species to water deficits [e.g. the

636   different fir species located in humid mountain areas, (Camarero et al., 2011; Camarero

637   et al., 2018)].

638   Here, we also showed that climate aridity can partially explain the response of the

639   NDVI to the different SPEI time scales. In Spain, the range of the mean aridity recorded

640   by the mean land cover types is much lower than that observed at the global scale for

641   the world biomes (Vicente-Serrano et al., 2013). This might explain why there are no

642   clear patterns in the response of the land cover types to the aridity gradients and the

643   SPEI time scales at which the maximum correlation between the NDVI and SPEI is

644   found. Nevertheless, we found some seasonal differences between the cold and warm

645   seasons. In summer, the NDVI responds to longer SPEI time scales, as opposed to the

646   most humid forests that respond to shorter time scales. This stresses that – in addition to

647   aridity- the degree of vulnerability to different duration water deficits, which are well-

648   quantified using the drought time scales, may contribute to explaining the spatial

649   distribution of the main land cover types across Spain given different biophysical

650   conditions, but also the different strategies of vegetation types to cope with water stress

651   (Chaves et al., 2003; McDowell et al., 2008), which are strongly variable in complex

652   Mediterranean ecosystems.

653

654   **5. Conclusions**

The main conclusions of this study are:

- Vegetation activity over large parts of Spain is closely related to the interannual variability of drought.
- The response of vegetation activity to drought is more pronounced during the warm season, which is attributed to the phenology of vegetation under different land cover types.
- There are clear seasonal differences in the response of the NDVI to drought.
- Natural grasslands and sclerophyllous vegetation show an earlier response to drought.
- There is a control in the response of the NDVI to drought severity by the climatic aridity, which is partially controlled by the land cover.
- The response of the NDVI is highly dependent on the time scale at which drought is quantified although there are differences in this response, as a function of land cover types.

Acknowledgements

This work was supported by the research projects PCIN-2015-220, CGL2014-52135-C03-01 and CGL2017-82216-R financed by the Spanish Commission of Science and Technology and FEDER. IMDROFLOOD financed by the Water Works 2014 co-funded all of the European Commission and INDECIS, which is part of ERA4CS, an ERA-NET initiated by JPI Climate, and funded by FORMAS (Sweden), DLR (Germany), BMWFW(Austria), IFD (Denmark), MINECO(Spain) and ANR (France), with co-funding by the European Union (Grant 690462), FORWARD financed under the ERA-NET Cofund WaterWorks2015 Call EU and Innovation Fund Denmark (IFD). This ERA-NET is an integral part of the 2016 Joint Activities developed by the Water Challenges for a Changing World Joint Programme Initiative (Water JPI). Marina Peña-Gallardo was supported by the Spanish Ministry of Economy and Competitiveness

References

Abrams, M. D., Schultz, J. C. and Kleiner, K. W.: Ecophysiological responses in mesic versus xeric hardwood species to an early-season drought in central Pennsylvania, For. Sci., 36(4), 970–981, 1990.

Allen, C. D., Macalady, A. K., Chenchouni, H., Bachelet, D., McDowell, N., Vennetier, M., Kitzberger, T., Rigling, A., Breshears, D. D., Hogg, E. H. (T. ., Gonzalez, P., Fensham, R., Zhang, Z., Castro, J., Demidova, N., Lim, J.-H., Allard, G., Running, S. W., Semerci, A. and Cobb, N.: A global overview of drought and heat-induced tree mortality reveals emerging climate change risks for forests, For. Ecol. Manage., 259(4), 660–684, doi:10.1016/j.foreco.2009.09.001, 2010.

Allen, C. D., Breshears, D. D. and McDowell, N. G.: On underestimation of global vulnerability to tree mortality and forest die-off from hotter drought in the Anthropocene, Ecosphere, 6(8), doi:10.1890/ES15-00203.1, 2015.

Allen, R. G., Pereira, L. S., Raes, D. and Smith, M.: No Title, Crop Evapotranspiration Guidel. Comput. Crop Water Requir., 1998.

697 Anyamba, A. and Tucker, C. J.: Analysis of Sahelian vegetation dynamics using
698 NOAA-AVHRR NDVI data from 1981-2003, J. Arid Environ., 63(3), 596–614,
699 doi:10.1016/j.jaridenv.2005.03.007, 2005.

700 Arzac, A., García-Cervigón, A. I., Vicente-Serrano, S. M., Loidi, J. and Olano, J. M.:
701 Phenological shifts in climatic response of secondary growth allow Juniperus sabina L.
702 to cope with altitudinal and temporal climate variability, Agric. For. Meteorol., 217,
703 doi:10.1016/j.agrformet.2015.11.011, 2016.

704 Asseng, S., Ewert, F., Martre, P., Rötter, R. P., Lobell, D. B., Cammarano, D., Kimball,
705 B. A., Ottman, M. J., Wall, G. W., White, J. W., Reynolds, M. P., Alderman, P. D.,
706 Prasad, P. V. V., Aggarwal, P. K., Anothai, J., Basso, B., Biernath, C., Challinor, A. J.,
707 De Sanctis, G., Doltra, J., Fereres, E., Garcia-Vila, M., Gayler, S., Hoogenboom, G.,
708 Hunt, L. A., Izaurralde, R. C., Jabloun, M., Jones, C. D., Kersebaum, K. C., Koehler,
709 A.-K., Müller, C., Naresh Kumar, S., Nendel, C., O'leary, G., Olesen, J. E., Palosuo, T.,
710 Priesack, E., Eyshi Rezaei, E., Ruane, A. C., Semenov, M. A., Shcherbak, I., Stöckle,
711 C., Stratonovitch, P., Streck, T., Supit, I., Tao, F., Thorburn, P. J., Waha, K., Wang, E.,
712 Wallach, D., Wolf, J., Zhao, Z. and Zhu, Y.: Rising temperatures reduce global wheat
713 production, Nat. Clim. Chang., 5(2), 143–147, doi:10.1038/nclimate2470, 2015.

714 Austin, R. B., Cantero-Martínez, C., Arrúe, J. L., Playán, E. and Cano-Marcellán, P.:
715 Yield-rainfall relationships in cereal cropping systems in the Ebro river valley of Spain,
716 Eur. J. Agron., 8(3–4), 239–248, doi:10.1016/S1161-0301(97)00063-4, 1998.

717 Bachmair, S., Kohn, I. and Stahl, K.: Exploring the link between drought indicators and
718 impacts, Nat. Hazards Earth Syst. Sci., 15(6), 1381–1397, doi:10.5194/nhess-15-1381-
719 2015, 2015.

720 Bachmair, S., Tanguy, M., Hannaford, J. and Stahl, K.: How well do meteorological
721 indicators represent agricultural and forest drought across Europe?, Environ. Res. Lett.,
722 13(3), doi:10.1088/1748-9326/aaafda, 2018.

723 Bailing, M., Zhiyong, L., Cunzhu, L., Lixin, W., Chengzhen, J., Fuxiang, B. and Chao,
724 J.: Temporal and spatial heterogeneity of drought impact on vegetation growth on the
725 Inner Mongolian Plateau, Rangel. J., 40(2), 113–128, doi:10.1071/RJ16097, 2018.

726 Baldocchi, D. D., Xu, L. and Kiang, N.: How plant functional-type, weather, seasonal
727 drought, and soil physical properties alter water and energy fluxes of an oak-grass
728 savanna and an annual grassland, Agric. For. Meteorol., 123(1–2), 13–39,
729 doi:10.1016/j.agrformet.2003.11.006, 2004.

730 Barbosa, H. A., Huete, A. R. and Baethgen, W. E.: A 20-year study of NDVI variability
731 over the Northeast Region of Brazil, J. Arid Environ., 67(2), 288–307,
732 doi:10.1016/j.jaridenv.2006.02.022, 2006.

733 Barker, L. J., Hannaford, J., Chiverton, A. and Svensson, C.: From meteorological to
734 hydrological drought using standardised indicators, Hydrol. Earth Syst. Sci., 20(6),
735 2483–2505, doi:10.5194/hess-20-2483-2016, 2016.

736 del Barrio, G., Puigdefabregas, J., Sanjuan, M. E., Stellmes, M. and Ruiz, A.:
737 Assessment and monitoring of land condition in the Iberian Peninsula, 1989-2000,
738 Remote Sens. Environ., 114(8), 1817–1832, doi:10.1016/j.rse.2010.03.009, 2010.

739 Berg, A., Sheffield, J. and Milly, P. C. D.: Divergent surface and total soil moisture
740 projections under global warming, Geophys. Res. Lett., 44(1), 236–244,
741 doi:10.1002/2016GL071921, 2017.

Bhuiyan, C., Singh, R. P. and Kogan, F. N.: Monitoring drought dynamics in the Aravalli region (India) using different indices based on ground and remote sensing data, Int. J. Appl. Earth Obs. Geoinf., 8(4), 289–302, doi:10.1016/j.jag.2006.03.002, 2006.

Breshears, D. D., Cobb, N. S., Rich, P. M., Price, K. P., Allen, C. D., Balice, R. G., Romme, W. H., Kastens, J. H., Floyd, M. L., Belnap, J., Anderson, J. J., Myers, O. B. and Meyer, C. W.: Regional vegetation die-off in response to global-change-type drought, Proc. Natl. Acad. Sci. U. S. A., 102(42), 15144–15148, doi:10.1073/pnas.0505734102, 2005.

Camarero, J. J., Bigler, C., Linares, J. C. and Gil-Pelegrín, E.: Synergistic effects of past historical logging and drought on the decline of Pyrenean silver fir forests, For. Ecol. Manage., 262(5), 759–769, doi:10.1016/j.foreco.2011.05.009, 2011.

Camarero, J. J., Gazol, A., Sangüesa-Barreda, G., Oliva, J. and Vicente-Serrano, S. M.: To die or not to die: Early warnings of tree dieback in response to a severe drought, J. Ecol., 103(1), doi:10.1111/1365-2745.12295, 2015.

Camarero, J. J., Gazol, A., Sangüesa-Barreda, G., Cantero, A., Sánchez-Salguero, R., Sánchez-Miranda, A., Granda, E., Serra-Maluquer, X. and Ibáñez, R.: Forest growth responses to drought at short- and long-term scales in Spain: Squeezing the stress memory from tree rings, Front. Ecol. Evol., 6(FEB), doi:10.3389/fevo.2018.00009, 2018.

Carlson, T. N. and Ripley, D. A.: On the relation between NDVI, fractional vegetation cover, and leaf area index, Remote Sens. Environ., 62(3), 241–252, doi:10.1016/S0034-4257(97)00104-1, 1997.

Carnicer, J., Coll, M., Ninyerola, M., Pons, X., Sánchez, G. and Peñuelas, J.: Widespread crown condition decline, food web disruption, and amplified tree mortality with increased climate change-type drought, Proc. Natl. Acad. Sci. U. S. A., 108(4), 1474–1478, doi:10.1073/pnas.1010070108, 2011.

Castro-Díez, P., Villar-Salvador, P., Pérez-Rontomé, C., Maestro-Martínez, M. and Montserrat-Martí, G.: Leaf morphology and leaf chemical composition in three Quercus (Fagaceae) species along a rainfall gradient in NE Spain, Trees - Struct. Funct., 11(3), 127–134, doi:10.1007/s004680050068, 1997.

Changnon, S. A. and Easterling, W. E.: MEASURING DROUGHT IMPACTS: THE ILLINOIS CASE, JAWRA J. Am. Water Resour. Assoc., 25(1), 27–42, doi:10.1111/j.1752-1688.1989.tb05663.x, 1989.

Chaves, M. M., Maroco, J. P. and Pereira, J. S.: Understanding plant responses to drought - From genes to the whole plant, Funct. Plant Biol., 30(3), 239–264, doi:10.1071/FP02076, 2003.

Ciais, P., Reichstein, M., Viovy, N., Granier, A., Ogée, J., Allard, V., Aubinet, M., Buchmann, N., Bernhofer, C., Carrara, A., Chevallier, F., De Noblet, N., Friend, A. D., Friedlingstein, P., Grünwald, T., Heinesch, B., Keronen, P., Knohl, A., Krinner, G., Loustau, D., Manca, G., Matteucci, G., Miglietta, F., Ourcival, J. M., Papale, D., Pilegaard, K., Rambal, S., Seufert, G., Soussana, J. F., Sanz, M. J., Schulze, E. D., Vesala, T. and Valentini, R.: Europe-wide reduction in primary productivity caused by the heat and drought in 2003, Nature, 437(7058), 529–533, doi:10.1038/nature03972, 2005.

Contreras, S. and Hunink, J. E.: Drought effects on rainfed agriculture using

787 standardized indices: A case study in SE Spain, in Drought: Research and Science-
788 Policy Interfacing - Proceedings of the International Conference on Drought: Research
789 and Science-Policy Interfacing, pp. 65–70., 2015.

790 Dardel, C., Kergoat, L., Hiernaux, P., Mougin, E., Grippa, M. and Tucker, C. J.: Re-
791 greening Sahel: 30 years of remote sensing data and field observations (Mali, Niger),
792 Remote Sens. Environ., 140, 350–364, doi:10.1016/j.rse.2013.09.011, 2014.

793 FAO: Food and Agricultural Organization, [online] Available from: http://www.fao.org
794 (Accessed 1 October 2018), 2018.

795 Fischer, E. M., Seneviratne, S. I., Vidale, P. L., Lüthi, D. and Schär, C.: Soil moisture-
796 atmosphere interactions during the 2003 European summer heat wave, J. Clim., 20(20),
797 5081–5099, doi:10.1175/JCLI4288.1, 2007.

798 García-Haro, F. J., Campos-Taberner, M., Sabater, N., Belda, F., Moreno, A., Gilabert,
799 M. A., Martínez, B., Pérez-Hoyos, A. and Meliá, J.: Vegetation vulnerability to drought
800 in Spain | Vulnerabilidad de la vegetación a la sequía en España, Rev. Teledetec., (42),
801 29–37, doi:10.4995/raet.2014.2283, 2014.

802 García, M., Litago, J., Palacios-Orueta, A., Pinzón, J. E. and Ustin Susan, L.: Short-term
803 propagation of rainfall perturbations on terrestrial ecosystems in central California,
804 Appl. Veg. Sci., 13(2), 146–162, doi:10.1111/j.1654-109X.2009.01057.x, 2010.

805 Gazol, A., Camarero, J. J., Anderegg, W. R. L. and Vicente-Serrano, S. M.: Impacts of
806 droughts on the growth resilience of Northern Hemisphere forests, Glob. Ecol.
807 Biogeogr., 26(2), doi:10.1111/geb.12526, 2017.

808 Gazol, A., Camarero, J. J., Vicente-Serrano, S. M., Sánchez-Salguero, R., Gutiérrez, E.,
809 de Luis, M., Sangüesa-Barreda, G., Novak, K., Rozas, V., Tíscar, P. A., Linares, J. C.,
810 Martín-Hernández, N., Martínez del Castillo, E., Ribas, M., García-González, I., Silla,
811 F., Camisón, A., Génova, M., Olano, J. M., Longares, L. A., Hevia, A., Tomás-
812 Burguera, M. and Galván, J. D.: Forest resilience to drought varies across biomes, Glob.
813 Chang. Biol., 24(5), doi:10.1111/gcb.14082, 2018.

814 Gessner, U., Naeimi, V., Klein, I., Kuenzer, C., Klein, D. and Dech, S.: The relationship
815 between precipitation anomalies and satellite-derived vegetation activity in Central
816 Asia, Glob. Planet. Change, 110, 74–87, doi:10.1016/j.gloplacha.2012.09.007, 2013.

817 González-Alonso, F. and Casanova, J. L.: Application of NOAA-AVHRR images for
818 the validation and risk assessment of natural disasters in Spain, in Remote Sensing '96,
819 pp. 227–233, Balkema, Rotterdam., 1997.

820 González-Hidalgo, J. C., Vicente-Serrano, S. M., Peña-Angulo, D., Salinas, C., Tomas-
821 Burguera, M. and Beguería, S.: High-resolution spatio-temporal analyses of drought
822 episodes in the western Mediterranean basin (Spanish mainland, Iberian Peninsula),
823 Acta Geophys., 66(3), doi:10.1007/s11600-018-0138-x, 2018.

824 Gouveia, C. M., Bastos, A., Trigo, R. M. and Dacamara, C. C.: Drought impacts on
825 vegetation in the pre- and post-fire events over Iberian Peninsula, Nat. Hazards Earth
826 Syst. Sci., 12(10), 3123–3137, doi:10.5194/nhess-12-3123-2012, 2012.

827 Gouveia, C. M., Páscoa, P., Russo, A. and Trigo, R. M.: Land degradation trend
828 assessment over iberia during 1982-2012 | Evaluación de la tendencia a la degradación
829 del suelo en Iberia durante 1982-2012, Cuad. Investig. Geogr., 42(1), 89–112,
830 doi:10.18172/cig.2808, 2016.

831 Gouveia, C. M., Trigo, R. M., Beguería, S. and Vicente-Serrano, S. M.: Drought

832 impacts on vegetation activity in the Mediterranean region: An assessment using remote
833 sensing data and multi-scale drought indicators, Glob. Planet. Change, 151,
834 doi:10.1016/j.gloplacha.2016.06.011, 2017.

835 Grissino-Mayer, H. D. and Fritts, H. C.: The International Tree-Ring Data Bank: An
836 enhanced global database serving the global scientific community, Holocene, 7(2), 235–
837 238, doi:10.1177/095968369700700212, 1997.

838 Gu, Y., Brown, J. F., Verdin, J. P. and Wardlow, B.: A five-year analysis of MODIS
839 NDVI and NDWI for grassland drought assessment over the central Great Plains of the
840 United States, Geophys. Res. Lett., 34(6), doi:10.1029/2006GL029127, 2007.

841 Herrmann, S. M., Anyamba, A. and Tucker, C. J.: Recent trends in vegetation dynamics
842 in the African Sahel and their relationship to climate, Glob. Environ. Chang., 15(4),
843 394–404, doi:10.1016/j.gloenvcha.2005.08.004, 2005.

844 Herrmann, S. M., Didan, K., Barreto-Munoz, A. and Crimmins, M. A.: Divergent
845 responses of vegetation cover in Southwestern US ecosystems to dry and wet years at
846 different elevations, Environ. Res. Lett., 11(12), doi:10.1088/1748-9326/11/12/124005,
847 2016.

848 Hill, J., Stellmes, M., Udelhoven, T., Röder, A. and Sommer, S.: Mediterranean
849 desertification and land degradation. Mapping related land use change syndromes based
850 on satellite observations, Glob. Planet. Change, 64(3–4), 146–157,
851 doi:10.1016/j.gloplacha.2008.10.005, 2008.

852 Hirschi, M., Seneviratne, S. I., Alexandrov, V., Boberg, F., Boroneant, C., Christensen,
853 O. B., Formayer, H., Orlowsky, B. and Stepanek, P.: Observational evidence for soil-
854 moisture impact on hot extremes in southeastern Europe, Nat. Geosci., 4(1), 17–21,
855 doi:10.1038/ngeo1032, 2011.

856 Huete, A., Didan, K., Miura, T., Rodriguez, E. P., Gao, X. and Ferreira, L. G.:
857 Overview of the radiometric and biophysical performance of the MODIS vegetation
858 indices, Remote Sens. Environ., 83(1–2), 195–213, doi:10.1016/S0034-4257(02)00096-
859 2, 2002.

860 Huxman, T. E., Smith, M. D., Fay, P. A., Knapp, A. K., Shaw, M. R., Lolk, M. E.,
861 Smith, S. D., Tissue, D. T., Zak, J. C., Weltzin, J. F., Pockman, W. T., Sala, O. E.,
862 Haddad, B. M., Harte, J., Koch, G. W., Schwinning, S., Small, E. E. and Williams, D.
863 G.: Convergence across biomes to a common rain-use efficiency, Nature, 429(6992),
864 651–654, doi:10.1038/nature02561, 2004.

865 Iglesias, E., Garrido, A. and Gómez-Ramos, A.: Evaluation of drought management in
866 irrigated areas, Agric. Econ., 29(2), 211–229, doi:10.1016/S0169-5150(03)00084-7,
867 2003.

868 Ivits, E., Horion, S., Fensholt, R. and Cherlet, M.: Drought footprint on European
869 ecosystems between 1999 and 2010 assessed by remotely sensed vegetation phenology
870 and productivity, Glob. Chang. Biol., 20(2), 581–593, doi:10.1111/gcb.12393, 2014.

871 Jenkins, J. C., Chojnacky, D. C., Heath, L. S. and Birdsey, R. A.: National-scale
872 biomass estimators for United States tree species, For. Sci., 49(1), 12–35, 2003.

873 Ji, L. and Peters, A. J.: Assessing vegetation response to drought in the northern Great
874 Plains using vegetation and drought indices, Remote Sens. Environ., 87(1), 85–98,
875 doi:10.1016/S0034-4257(03)00174-3, 2003.

876 Julien, Y., Sobrino, J. A., Mattar, C., Ruescas, A. B., Jiménez-Muñoz, J. C., Sòria, G.,

877 Hidalgo, V., Atitar, M., Franch, B. and Cuenca, J.: Temporal analysis of normalized
878 difference vegetation index (NDVI) and land surface temperature (LST) parameters to
879 detect changes in the Iberian land cover between 1981 and 2001, Int. J. Remote Sens.,
880 32(7), 2057–2068, doi:10.1080/01431161003762363, 2011.

881 De Keersmaecker, W., Lhermitte, S., Hill, M. J., Tits, L., Coppin, P. and Somers, B.:
882 Assessment of regional vegetation response to climate anomalies: A case study for
883 australia using GIMMS NDVI time series between 1982 and 2006, Remote Sens., 9(1),
884 doi:10.3390/rs9010034, 2017.

885 Knipling, E. B.: Physical and physiological basis for the reflectance of visible and near-
886 infrared radiation from vegetation, Remote Sens. Environ., 1(3), 155–159,
887 doi:10.1016/S0034-4257(70)80021-9, 1970.

888 Kogan, F. N.: Global Drought Watch from Space, Bull. Am. Meteorol. Soc., 78(4),
889 621–636, doi:10.1175/1520-0477(1997)078<0621:GDWFS>2.0.CO;2, 1997.

890 Lasanta, T. and Vicente-Serrano, S. M.: Complex land cover change processes in
891 semiarid Mediterranean regions: An approach using Landsat images in northeast Spain,
892 Remote Sens. Environ., 124, doi:10.1016/j.rse.2012.04.023, 2012.

893 Lasanta, T., Arnáez, J., Pascual, N., Ruiz-Flaño, P., Errea, M. P. and Lana-Renault, N.:
894 Space–time process and drivers of land abandonment in Europe, Catena, 149, 810–823,
895 doi:10.1016/j.catena.2016.02.024, 2017.

896 Liu, N., Harper, R. J., Dell, B., Liu, S. and Yu, Z.: Vegetation dynamics and rainfall
897 sensitivity for different vegetation types of the Australian continent in the dry period
898 2002–2010, Ecohydrology, 10(2), doi:10.1002/eco.1811, 2017.

899 Liu, W. T. and Kogan, F. N.: Monitoring regional drought using the vegetation
900 condition index, Int. J. Remote Sens., 17(14), 2761–2782,
901 doi:10.1080/01431169608949106, 1996.

902 Lloret, F., Lobo, A., Estevan, H., Maisongrande, P., Vayreda, J. and Terradas, J.:
903 Woody plant richness and NDVI response to drought events in Catalonian (northeastern
904 Spain) forests, Ecology, 88(9), 2270–2279, doi:10.1890/06-1195.1, 2007.

905 Lobell, D. B., Hammer, G. L., Chenu, K., Zheng, B., Mclean, G. and Chapman, S. C.:
906 The shifting influence of drought and heat stress for crops in northeast Australia, Glob.
907 Chang. Biol., 21(11), 4115–4127, doi:10.1111/gcb.13022, 2015.

908 López-Moreno, J. I., Beguería, S. and García-Ruiz, J. M.: The management of a large
909 Mediterranean reservoir: Storage regimens of the Yesa Reservoir, Upper Aragon River
910 basin, Central Spanish Pyrenees, Environ. Manage., 34(4), 508–515,
911 doi:10.1007/s00267-003-0249-1, 2004.

912 López-Moreno, J. I., Vicente-Serrano, S. M., Zabalza, J., Beguería, S., Lorenzo-Lacruz,
913 J., Azorin-Molina, C. and Morán-Tejeda, E.: Hydrological response to climate
914 variability at different time scales: A study in the Ebro basin, J. Hydrol., 477, 175–188,
915 doi:10.1016/j.jhydrol.2012.11.028, 2013.

916 Lorenzo-Lacruz, J., Vicente-Serrano, S. M., López-Moreno, J. I., Beguería, S., García-
917 Ruiz, J. M. and Cuadrat, J. M.: The impact of droughts and water management on
918 various hydrological systems in the headwaters of the Tagus River (central Spain), J.
919 Hydrol., 386(1–4), doi:10.1016/j.jhydrol.2010.01.001, 2010.

920 Lorenzo-Lacruz, J., Morán-Tejeda, E., Vicente-Serrano, S. M. and López-Moreno, J. I.:
921 Streamflow droughts in the Iberian Peninsula between 1945 and 2005: Spatial and

922   temporal patterns, Hydrol. Earth Syst. Sci., 17(1), doi:10.5194/hess-17-119-2013, 2013.

923   Lotsch, A., Friedl, M. A., Anderson, B. T. and Tucker, C. J.: Coupled vegetation-
924   precipitation variability observed from satellite and climate records, Geophys. Res.
925   Lett., 30(14), doi:10.1029/2003GL017506, 2003.

926   Ma, X., Huete, A., Moran, S., Ponce-Campos, G. and Eamus, D.: Abrupt shifts in
927   phenology and vegetation productivity under climate extremes, J. Geophys. Res.
928   Biogeosciences, 120(10), 2036–2052, doi:10.1002/2015JG003144, 2015.

929   Malo, A. R. and Nicholson, S. E.: A study of rainfall and vegetation dynamics in the
930   African Sahel using normalized difference vegetation index, J. Arid Environ., 19(1), 1–
931   24, 1990.

932   Martínez-Fernández, J. and Ceballos, A.: Temporal Stability of Soil Moisture in a
933   Large-Field Experiment in Spain, Soil Sci. Soc. Am. J., 67(6), 1647–1656, 2003.

934   McDowell, N., Pockman, W. T., Allen, C. D., Breshears, D. D., Cobb, N., Kolb, T.,
935   Plaut, J., Sperry, J., West, A., Williams, D. G. and Yepez, E. A.: Mechanisms of plant
936   survival and mortality during drought: Why do some plants survive while others
937   succumb to drought?, New Phytol., 178(4), 719–739, doi:10.1111/j.1469-
938   8137.2008.02436.x, 2008.

939   McKee, T. B., Doesken, N. J. and Kleist, J.: The relationship of drought frequency and
940   duration to time scales, Eighth Conf. Appl. Climatol., 179–184, 1993.

941   Milich, L. and Weiss, E.: Characterization of the sahel: Implications of correctly
942   calculating interannual coefficients of variation (CoVs) from GAC NDVI values, Int. J.
943   Remote Sens., 18(18), 3749–3759, doi:10.1080/014311697216603, 1997.

944   Molina, A. J. and del Campo, A. D.: The effects of experimental thinning on throughfall
945   and stemflow: A contribution towards hydrology-oriented silviculture in Aleppo pine
946   plantations, For. Ecol. Manage., 269, 206–213, doi:10.1016/j.foreco.2011.12.037, 2012.

947   Mu, Q., Zhao, M., Kimball, J. S., McDowell, N. G. and Running, S. W.: A remotely
948   sensed global terrestrial drought severity index, Bull. Am. Meteorol. Soc., 94(1), 83–98,
949   doi:10.1175/BAMS-D-11-00213.1, 2013.

950   Mühlbauer, S., Costa, A. C. and Caetano, M.: A spatiotemporal analysis of droughts and
951   the influence of North Atlantic Oscillation in the Iberian Peninsula based on MODIS
952   imagery, Theor. Appl. Climatol., 124(3–4), 703–721, doi:10.1007/s00704-015-1451-9,
953   2016.

954   Mukherjee, S., Mishra, A. and Trenberth, K. E.: Climate Change and Drought: a
955   Perspective on Drought Indices, Curr. Clim. Chang. Reports, 4(2), 145–163,
956   doi:10.1007/s40641-018-0098-x, 2018.

957   Myneni, R. B., Hall, F. G., Sellers, P. J. and Marshak, A. L.: Interpretation of spectral
958   vegetation indexes, IEEE Trans. Geosci. Remote Sens., 33(2), 481–486,
959   doi:10.1109/36.377948, 1995.

960   Newberry, T. L.: Effect of climatic variability on δ^{13}C and tree-ring growth in piñon
961   pine (Pinus edulis), Trees - Struct. Funct., 24(3), 551–559, doi:10.1007/s00468-010-
962   0426-9, 2010.

963   Nicholson, S. E., Davenport, M. L. and Malo, A. R.: A comparison of the vegetation
964   response to rainfall in the Sahel and East Africa, using normalized difference vegetation
965   index from NOAA AVHRR, Clim. Change, 17(2–3), 209–241,

966   doi:10.1007/BF00138369, 1990.

967   Okin, G. S., Dong, C., Willis, K. S., Gillespie, T. W. and MacDonald, G. M.: The
968   Impact of Drought on Native Southern California Vegetation: Remote Sensing Analysis
969   Using MODIS-Derived Time Series, J. Geophys. Res. Biogeosciences, 123(6), 1927–
970   1939, doi:10.1029/2018JG004485, 2018.

971   Olsen, J. L., Ceccato, P., Proud, S. R., Fensholt, R., Grippa, M., Mougin, B., Ardö, J.
972   and Sandholt, I.: Relation between seasonally detrended shortwave infrared reflectance
973   data and land surface moisture in semi-arid Sahel, Remote Sens., 5(6), 2898–2927,
974   doi:10.3390/rs5062898, 2013.

975   Páscoa, P., Gouveia, C. M., Russo, A. and Trigo, R. M.: The role of drought on wheat
976   yield interannual variability in the Iberian Peninsula from 1929 to 2012, Int. J.
977   Biometeorol., 61(3), 439–451, doi:10.1007/s00484-016-1224-x, 2017.

978   Pasho, E., Camarero, J. J., de Luis, M. and Vicente-Serrano, S. M.: Impacts of drought
979   at different time scales on forest growth across a wide climatic gradient in north-eastern
980   Spain, Agric. For. Meteorol., 151(12), doi:10.1016/j.agrformet.2011.07.018, 2011.

981   Pausas, J. G.: Changes in fire and climate in the eastern Iberian Peninsula
982   (Mediterranean Basin), Clim. Change, 63(3), 337–350,
983   doi:10.1023/B:CLIM.0000018508.94901.9c, 2004.

984   Pausas, J. G. and Fernández-Muñoz, S.: Fire regime changes in the Western
985   Mediterranean Basin: From fuel-limited to drought-driven fire regime, Clim. Change,
986   110(1–2), 215–226, doi:10.1007/s10584-011-0060-6, 2012.

987   Peco, B., Ortega, M. and Levassor, C.: Similarity between seed bank and vegetation in
988   Mediterranean grassland: A predictive model, J. Veg. Sci., 9(6), 815–828,
989   doi:10.2307/3237047, 1998.

990   Peña-Gallardo, M., Vicente-Serrano, S. M., Camarero, J. J., Gazol, A., Sánchez-
991   Salguero, R., Domínguez-Castro, F., El Kenawy, A., Beguería-Portugés, S., Gutiérrez,
992   E., de Luis, M., Sangüesa-Barreda, G., Novak, K., Rozas, V., Tíscar, P. A., Linares, J.
993   C., del Castillo, E., Ribas Matamoros, M., García-González, I., Silla, F., Camisón, Á.,
994   Génova, M., Olano, J. M., Longares, L. A., Hevia, A. and Galván, J. D.: Drought
995   Sensitiveness on Forest Growth in Peninsular Spain and the Balearic Islands, Forests,
996   9(9), 2018a.

997   Peña-Gallardo, M., SM, V.-S., Domínguez-Castro, F., Quiring, S., Svoboda, M.,
998   Beguería, S. and Hannaford, J.: Effectiveness of drought indices in identifying impacts
999   on major crops across the USA , Clim. Res., 75(3), 221–240, 2018b.

1000   Pinzon, J. E. and Tucker, C. J.: A non-stationary 1981-2012 AVHRR
1001   NDVI<inf>3g</inf>time series, Remote Sens., 6(8), 6929–6960,
1002   doi:10.3390/rs6086929, 2014.

1003   Quiring, S. M. and Ganesh, S.: Evaluating the utility of the Vegetation Condition Index
1004   (VCI) for monitoring meteorological drought in Texas, Agric. For. Meteorol., 150(3),
1005   330–339, doi:10.1016/j.agrformet.2009.11.015, 2010.

1006   Quiroga, S. and Iglesias, A.: A comparison of the climate risks of cereal, citrus,
1007   grapevine and olive production in Spain, Agric. Syst., 101(1–2), 91–100,
1008   doi:10.1016/j.agsy.2009.03.006, 2009.

1009   Reichstein, M., Ciais, P., Papale, D., Valentini, R., Running, S., Viovy, N., Cramer, W.,
1010   Granier, A., Ogée, J., Allard, V., Aubinet, M., Bernhofer, C., Buchmann, N., Carrara,

1011   A., Grünwald, T., Heimann, M., Heinesch, B., Knohl, A., Kutsch, W., Loustau, D.,
1012   Manca, G., Matteucci, G., Miglietta, F., Ourcival, J. M., Pilegaard, K., Pumpanen, J.,
1013   Rambal, S., Schaphoff, S., Seufert, G., Soussana, J.-F., Sanz, M.-J., Vesala, T. and
1014   Zhao, M.: Reduction of ecosystem productivity and respiration during the European
1015   summer 2003 climate anomaly: A joint flux tower, remote sensing and modelling
1016   analysis, Glob. Chang. Biol., 13(3), 634–651, doi:10.1111/j.1365-2486.2006.01224.x,
1017   2007.

1018   Restaino, C. M., Peterson, D. L. and Littell, J.: Increased water deficit decreases
1019   Douglas fir growth throughout western US forests, Proc. Natl. Acad. Sci. U. S. A.,
1020   113(34), 9557–9562, doi:10.1073/pnas.1602384113, 2016.

1021   Rhee, J., Im, J. and Carbone, G. J.: Monitoring agricultural drought for arid and humid
1022   regions using multi-sensor remote sensing data, Remote Sens. Environ., 114(12), 2875–
1023   2887, doi:10.1016/j.rse.2010.07.005, 2010.

1024   Russi, L., Cocks, P. S. and Roberts, E. H.: Seed bank dynamics in a Mediterranean
1025   grassland, J. Appl. Ecol., 29(3), 763–771, doi:10.2307/2404486, 1992.

1026   Scaini, A., Sánchez, N., Vicente-Serrano, S. M. and Martínez-Fernández, J.: SMOS-
1027   derived soil moisture anomalies and drought indices: A comparative analysis using in
1028   situ measurements, Hydrol. Process., 29(3), doi:10.1002/hyp.10150, 2015.

1029   Schultz, P. A. and Halpert, M. S.: Global analysis of the relationships among a
1030   vegetation index, precipitation and land surface temperature, Int. J. Remote Sens.,
1031   16(15), 2755–2777, doi:10.1080/01431169508954590, 1995.

1032   Slayback, D. A., Pinzon, J. E., Los, S. O. and Tucker, C. J.: Northern hemisphere
1033   photosynthetic trends 1982-99, Glob. Chang. Biol., 9(1), 1–15, doi:10.1046/j.1365-
1034   2486.2003.00507.x, 2003.

1035   Sona, N. T., Chen, C. F., Chen, C. R., Chang, L. Y. and Minh, V. Q.: Monitoring
1036   agricultural drought in the lower mekong basin using MODIS NDVI and land surface
1037   temperature data, Int. J. Appl. Earth Obs. Geoinf., 18(1), 417–427,
1038   doi:10.1016/j.jag.2012.03.014, 2012.

1039   Stagge, J. H., Kohn, I., Tallaksen, L. M. and Stahl, K.: Modeling drought impact
1040   occurrence based on meteorological drought indices in Europe, J. Hydrol., 530, 37–50,
1041   doi:10.1016/j.jhydrol.2015.09.039, 2015.

1042   Stellmes, M., Röder, A., Udelhoven, T. and Hill, J.: Mapping syndromes of land change
1043   in Spain with remote sensing time series, demographic and climatic data, Land use
1044   policy, 30(1), 685–702, doi:10.1016/j.landusepol.2012.05.007, 2013.

1045   Tucker, C. J.: Red and photographic infrared linear combinations for monitoring
1046   vegetation, Remote Sens. Environ., 8(2), 127–150, doi:10.1016/0034-4257(79)90013-0,
1047   1979.

1048   Tucker, C. J., Pinzon, J. E., Brown, M. E., Slayback, D. A., Pak, E. W., Mahoney, R.,
1049   Vermote, E. F. and El Saleous, N.: An extended AVHRR 8-km NDVI dataset
1050   compatible with MODIS and SPOT vegetation NDVI data, Int. J. Remote Sens., 26(20),
1051   4485–4498, doi:10.1080/01431160500168686, 2005.

1052   Udelhoven, T., Stellmes, M., del Barrio, G. and Hill, J.: Assessment of rainfall and
1053   NDVI anomalies in Spain (1989-1999) using distributed lag models, Int. J. Remote
1054   Sens., 30(8), 1961–1976, doi:10.1080/01431160802546829, 2009.

1055   Vicente-Serrano, S. M.: Spatial and temporal analysis of droughts in the Iberian

Peninsula (1910-2000), Hydrol. Sci. J., 51(1), doi:10.1623/hysj.51.1.83, 2006.

Vicente-Serrano, S. M.: Evaluating the impact of drought using remote sensing in a Mediterranean, Semi-arid Region, Nat. Hazards, 40(1), doi:10.1007/s11069-006-0009-7, 2007.

Vicente-Serrano, S. M. and Beguería, S.: Comment on "Candidate distributions for climatological drought indices (SPI and SPEI)" by James H. Stagge et al., Int. J. Climatol., 36(4), doi:10.1002/joc.4474, 2016.

Vicente-Serrano, S. M., Cuadrat-Prats, J. M. and Romo, A.: Aridity influence on vegetation patterns in the middle Ebro Valley (Spain): Evaluation by means of AVHRR images and climate interpolation techniques, J. Arid Environ., 66(2), doi:10.1016/j.jaridenv.2005.10.021, 2006.

Vicente-Serrano, S. M., Beguería, S. and López-Moreno, J. I.: A multiscalar drought index sensitive to global warming: The standardized precipitation evapotranspiration index, J. Clim., 23(7), doi:10.1175/2009JCLI2909.1, 2010.

Vicente-Serrano, S. M., Beguería, S. and López-Moreno, J. I.: Comment on Characteristics and trends in various forms of the Palmer Drought Severity Index (PDSI) during 1900-2008 by Aiguo Dai, J. Geophys. Res. Atmos., 116(19), 2011.

Vicente-Serrano, S. M., Beguería, S., Lorenzo-Lacruz, J., Camarero, J. J., López-Moreno, J. I., Azorin-Molina, C., Revuelto, J., Morán-Tejeda, E. and Sanchez-Lorenzo, A.: Performance of drought indices for ecological, agricultural, and hydrological applications, Earth Interact., 16(10), doi:10.1175/2012EI000434.1, 2012.

Vicente-Serrano, S. M., Gouveia, C., Camarero, J. J., Beguería, S., Trigo, R., López-Moreno, J. I., Azorín-Molina, C., Pasho, E., Lorenzo-Lacruz, J., Revuelto, J., Morán-Tejeda, E. and Sanchez-Lorenzo, A.: Response of vegetation to drought time-scales across global land biomes, Proc. Natl. Acad. Sci. U. S. A., 110(1), doi:10.1073/pnas.1207068110, 2013.

Vicente-Serrano, S. M., Camarero, J. J. and Azorin-Molina, C.: Diverse responses of forest growth to drought time-scales in the Northern Hemisphere, Glob. Ecol. Biogeogr., 23(9), doi:10.1111/geb.12183, 2014a.

Vicente-Serrano, S. M., Lopez-Moreno, J.-I., Beguería, S., Lorenzo-Lacruz, J., Sanchez-Lorenzo, A., García-Ruiz, J. M., Azorin-Molina, C., Morán-Tejeda, E., Revuelto, J., Trigo, R., Coelho, F. and Espejo, F.: Evidence of increasing drought severity caused by temperature rise in southern Europe, Environ. Res. Lett., 9(4), doi:10.1088/1748-9326/9/4/044001, 2014b.

Vicente-Serrano, S. M., Azorin-Molina, C., Sanchez-Lorenzo, A., Revuelto, J., López-Moreno, J. I., González-Hidalgo, J. C., Moran-Tejeda, E. and Espejo, F.: Reference evapotranspiration variability and trends in Spain, 1961-2011, Glob. Planet. Change, 121, doi:10.1016/j.gloplacha.2014.06.005, 2014c.

Vicente-Serrano, S. M., Azorin-Molina, C., Sanchez-Lorenzo, A., Revuelto, J., Morán-Tejeda, E., Lõpez-Moreno, J. I. and Espejo, F.: Sensitivity of reference evapotranspiration to changes in meteorological parameters in Spain (1961-2011), Water Resour. Res., 50(11), doi:10.1002/2014WR015427, 2014d.

Vicente-Serrano, S. M., Cabello, D., Tomás-Burguera, M., Martín-Hernández, N., Beguería, S., Azorin-Molina, C. and Kenawy, A. E.: Drought variability and land degradation in semiarid regions: Assessment using remote sensing data and drought

1101   indices (1982-2011), Remote Sens., 7(4), doi:10.3390/rs70404391, 2015.

1102   Vicente-Serrano, S. M., Tomas-Burguera, M., Beguería, S., Reig, F., Latorre, B., Peña-
1103   Gallardo, M., Luna, M. Y., Morata, A. and González-Hidalgo, J. C.: A High Resolution
1104   Dataset of Drought Indices for Spain, Data, 2(3), 2017.

1105   Vicente-Serrano, S. M., Martín-Hernández, N., Reig, F., Azorin-Molina, C., Zabalza, J.,
1106   Beguería, S., Domínguez-Castro, F., El Kenawy, A., Peña-Gallardo, M., Noguera, I. and
1107   García, M.: Vegetation greening in Spain detected from long term data (1981-2015),
1108   Submitt. to Int. J. Remote Sens., 2018.

1109   Wan, Z., Wang, P. and Li, X.: Using MODIS Land Surface Temperature and
1110   Normalized Difference Vegetation Index products for monitoring drought in the
1111   southern Great Plains, USA, Int. J. Remote Sens., 25(1), 61–72,
1112   doi:10.1080/0143116031000115328, 2004.

1113   Wang, J., Rich, P. M. and Price, K. P.: Temporal responses of NDVI to precipitation
1114   and temperature in the central Great Plains, USA, Int. J. Remote Sens., 24(11), 2345–
1115   2364, doi:10.1080/01431160210154812, 2003.

1116   Xulu, S., Peerbhay, K., Gebreslasie, M. and Ismail, R.: Drought influence on forest
1117   plantations in Zululand, South Africa, using MODIS time series and climate data,
1118   Forests, 9(9), doi:10.3390/f9090528, 2018.

1119   Yang, S., Meng, D., Li, X. and Wu, X.: Multi-scale responses of vegetation changes
1120   relative to the SPEI meteorological drought index in North China in 2001-2014,
1121   Shengtai Xuebao/ Acta Ecol. Sin., 38(3), 1028–1039, doi:10.5846/stxb201611242398,
1122   2018.

1123   Zhang, L., Xiao, J., Zhou, Y., Zheng, Y., Li, J. and Xiao, H.: Drought events and their
1124   effects on vegetation productivity in China, Ecosphere, 7(12), doi:10.1002/ecs2.1591,
1125   2016.

1126   Zhang, Q., Kong, D., Singh, V. P. and Shi, P.: Response of vegetation to different time-
1127   scales drought across China: Spatiotemporal patterns, causes and implications, Glob.
1128   Planet. Change, 152, 1–11, doi:10.1016/j.gloplacha.2017.02.008, 2017.

1129   Zhao, M. and Running, S. W.: Drought-induced reduction in global terrestrial net
1130   primary production from 2000 through 2009, Science (80-.)., 329(5994), 940–943,
1131   doi:10.1126/science.1192666, 2010.

1132   Zhao, M., Geruo, A., Velicogna, I. and Kimball, J. S.: Satellite observations of regional
1133   drought severity in the continental United States using GRACE-based terrestrial water
1134   storage changes, J. Clim., 30(16), 6297–6308, doi:10.1175/JCLI-D-16-0458.1, 2017.

1135   Zhao, X., Wei, H., Liang, S., Zhou, T., He, B., Tang, B. and Wu, D.: Responses of
1136   natural vegetation to different stages of extreme drought during 2009-2010 in
1137   Southwestern China, Remote Sens., 7(10), 14039–14054, doi:10.3390/rs71014039,
1138   2015.

1139

1140
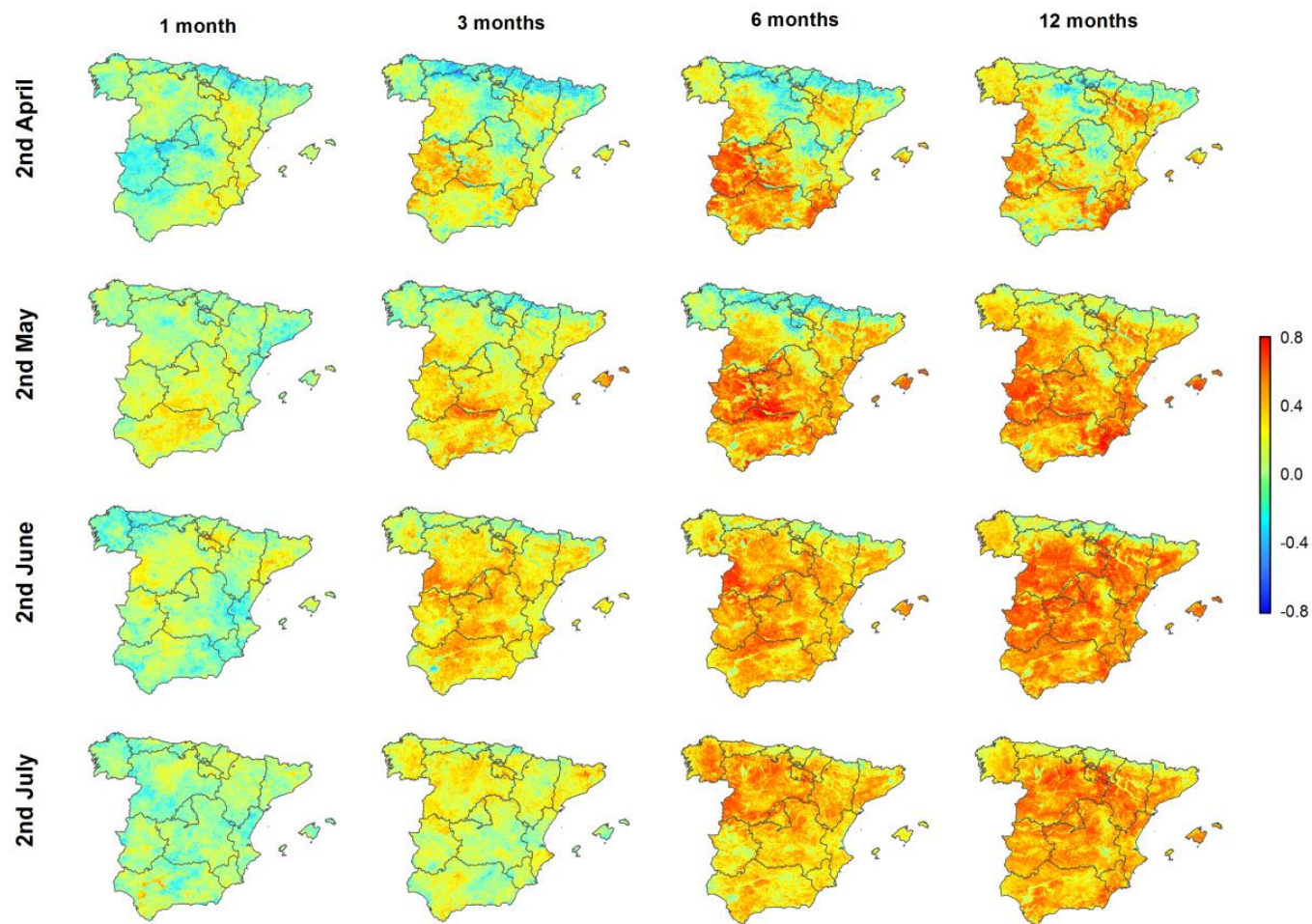
Figure 1: Spatial distribution of the Pearson's r correlation coefficient calculated between the sNDVI and different SPEI time scales for different
semi-monthly periods.

1141

1142

1143

1144
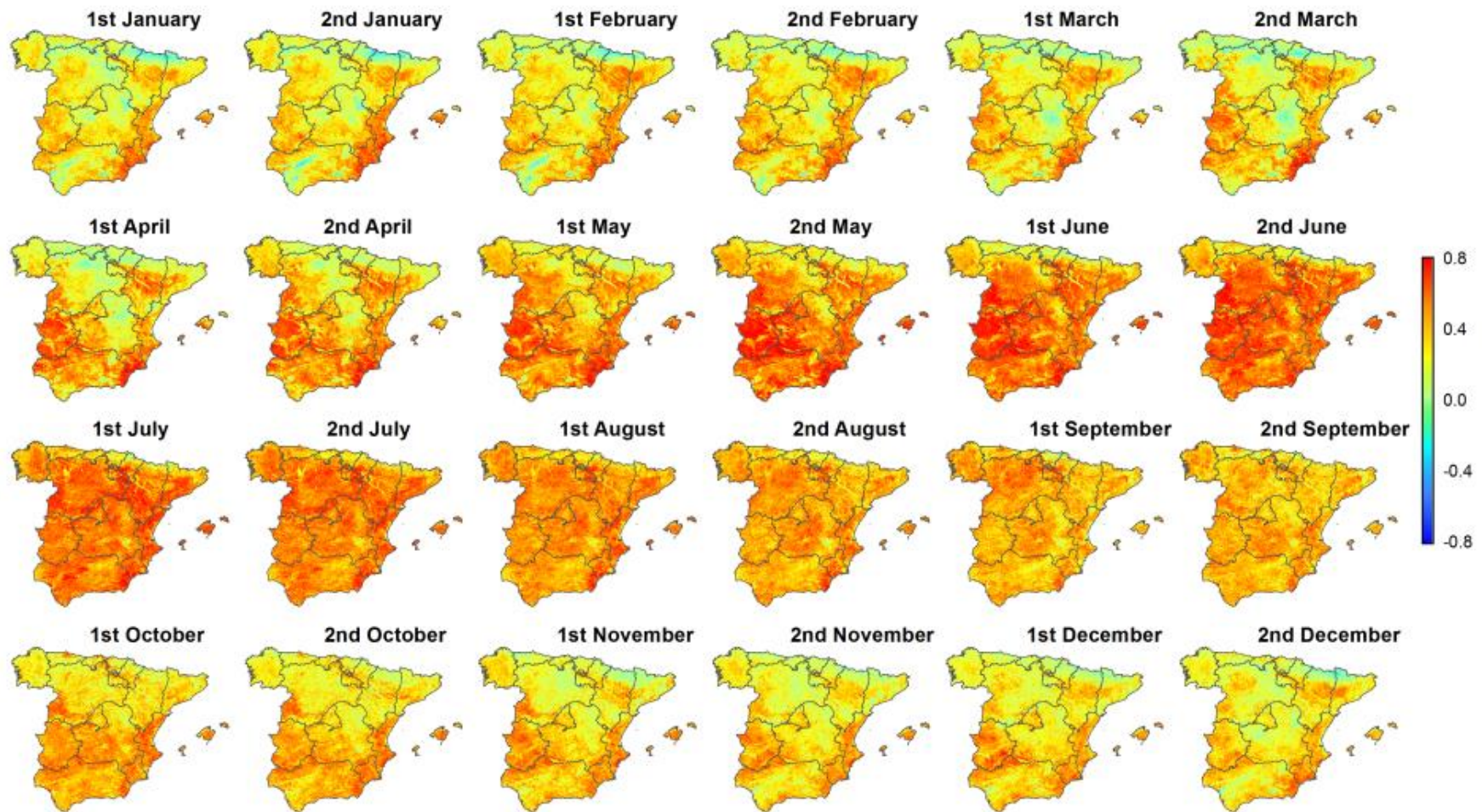
1145   Figure 2: Spatial distribution of the maximum correlation between the sNDVI and the SPEI during the different semi-monthly periods.

1146   Table 1: Percentage of the total surface area according to the different significance

1147   categories of Pearson's r correlations between the sNDVI and SPEI.

	Negative (p < 0.05)	Negative (p > 0.05)	Positive (p > 0.05)	Positive (p < 0.05)
1st Jan	0.3	9.8	41.3	48.6
2nd Jan	0.4	8.7	40.2	50.7
1st Feb	0.3	7.5	39.9	52.3
2nd Feb	0.1	7.5	39.0	53.4
1st Mar	0.2	8.9	41.6	49.4
2nd Mar	0.2	11.3	38.2	50.3
1st Apr	0.0	7.6	34.9	57.5
2nd Apr	0.0	3.4	27.0	69.7
1st May	0.0	1.6	19.0	79.4
2nd May	0.0	0.9	14.2	84.9
1st Jun	0.0	1.2	10.8	88.0
2nd Jun	0.0	0.5	7.4	92.0
1st Jul	0.0	0.3	5.3	94.4
2nd Jul	0.0	0.1	4.5	95.4
1st Aug	0.0	0.1	5.9	94.1
2nd Aug	0.0	0.2	10.6	89.2
1st Sep	0.0	0.6	14.0	85.4
2nd Sep	0.0	0.4	16.9	82.6
1st Oct	0.0	1.5	24.5	74.0
2nd Oct	0.0	1.9	31.1	67.0
1st Nov	0.0	4.5	35.6	59.8
2nd Nov	0.0	4.8	41.8	53.4
1st Dec	0.0	4.4	38.9	56.7
2nd Dec	0.2	5.9	43.1	50.8

1148

1149

1150
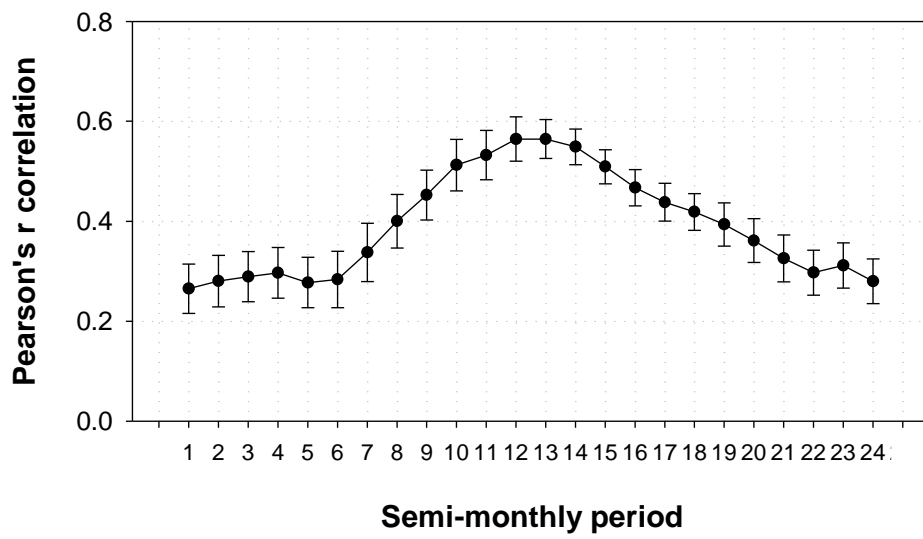
1151   Figure 3: Spatial Average and standard error of the Pearson's r correlation coefficient
1152   between the sNDVI and SPEI time series.

1153
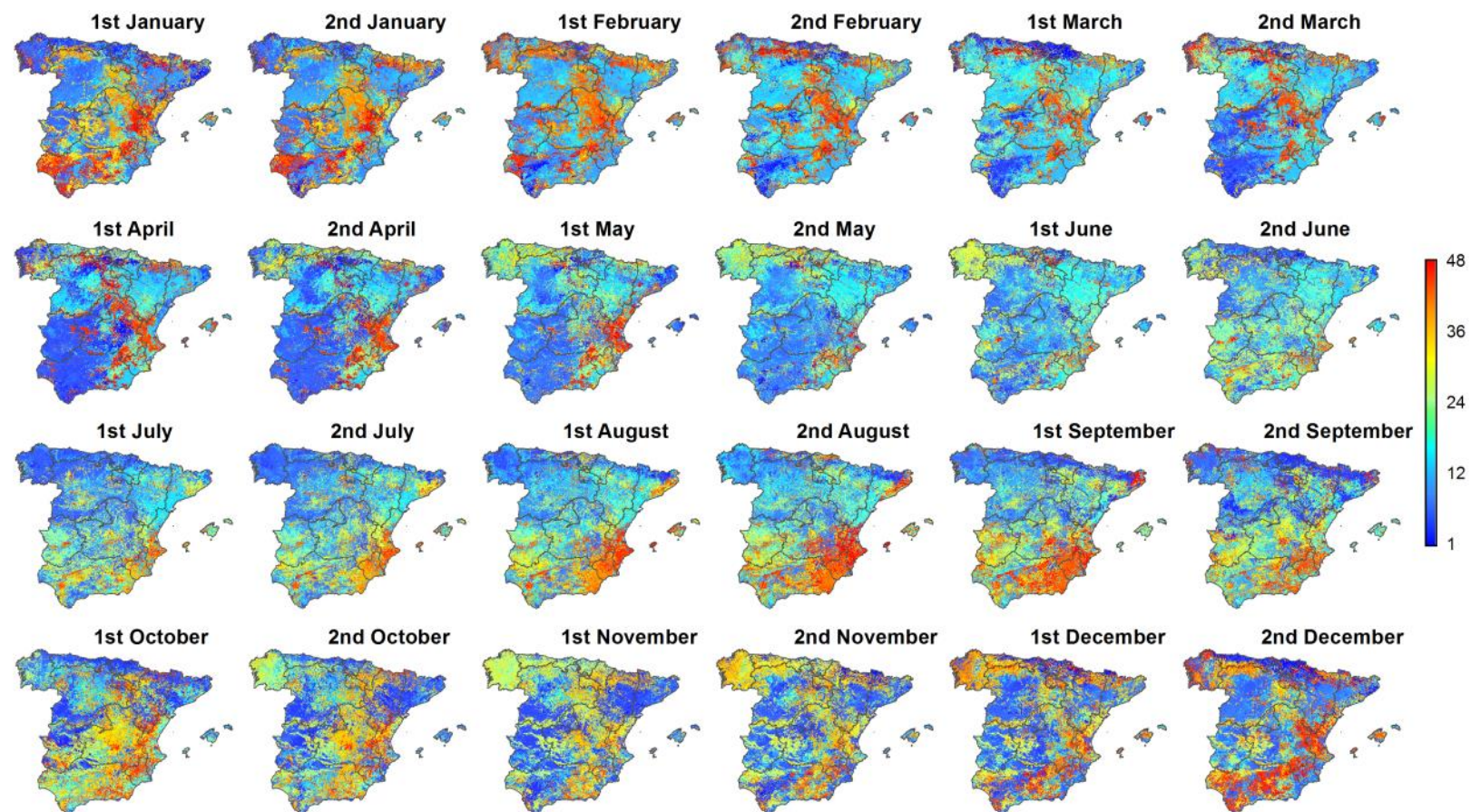
1154

Figure 4: Spatial distribution of the SPEI time scales at which the maximum correlation between the sNDVI and SPEI is found for each one of
the semi-monthly periods.

1155
1156
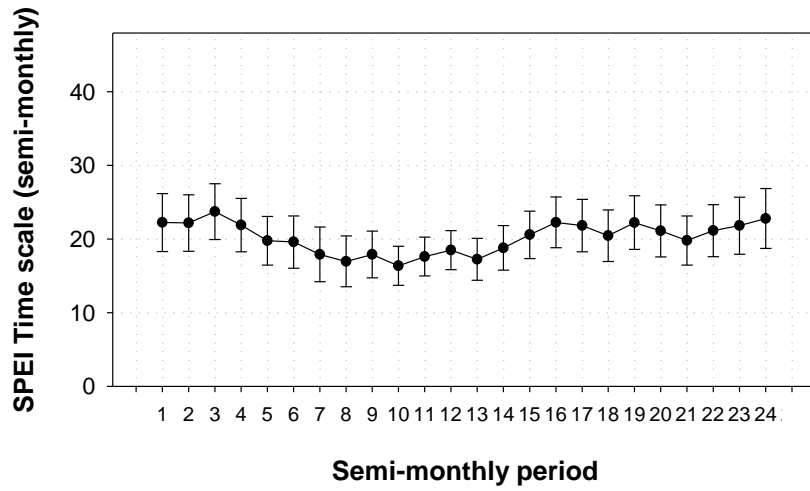
1157

1158   Figure 5: Average and standard error of the SPEI time scale at which the maximum
1159   Pearson's r correlation coefficient between the sNDVI and SPEI is found.

1160

1161
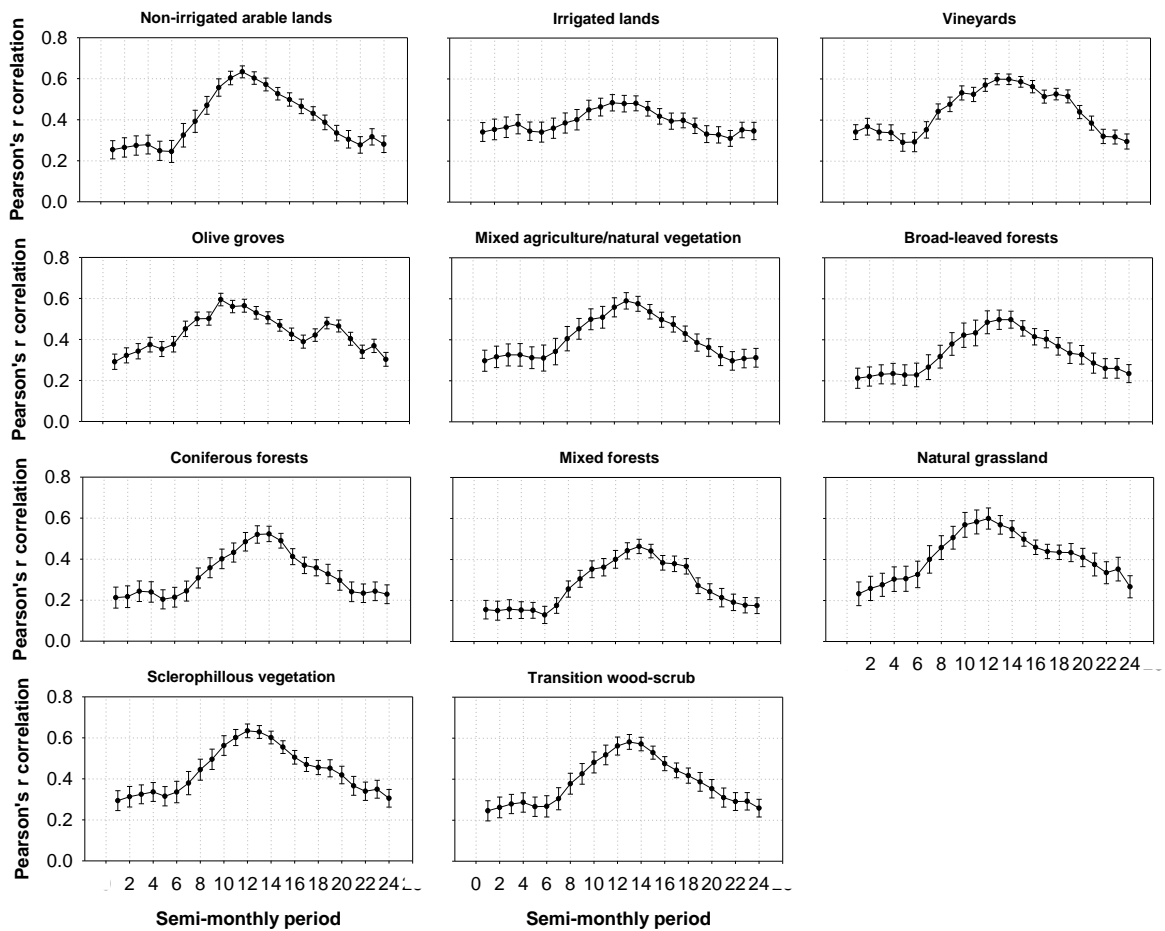
Figure 6: Average and standard error of the Pearson's r correlation coefficient between the sNDVI and SPEI for the different land cover types.
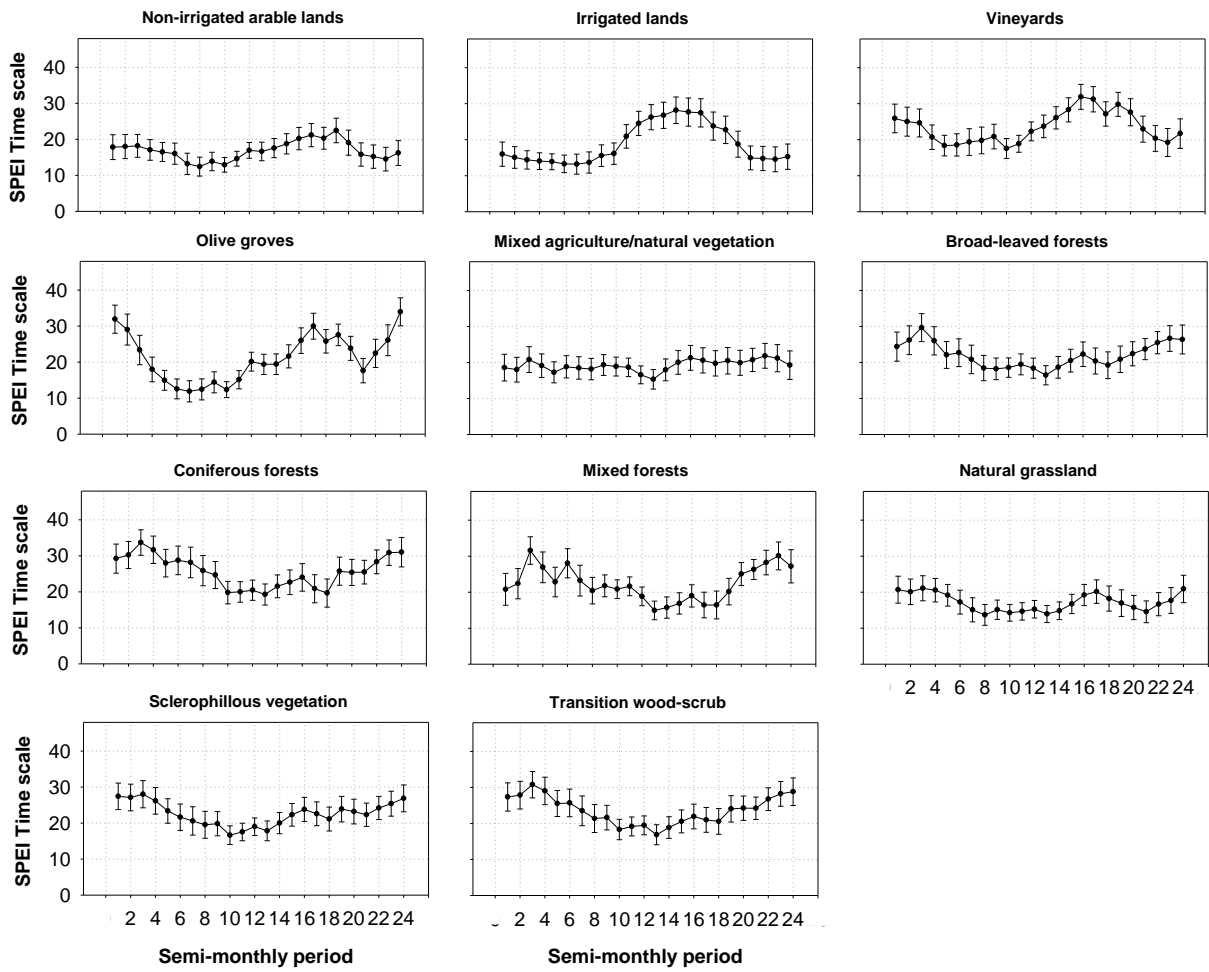
Figure 7: Average and standard error of the SPEI time scale at which the maximum Pearson's r correlation coefficient was found between the sNDVI and SPEI for the different land cover types.
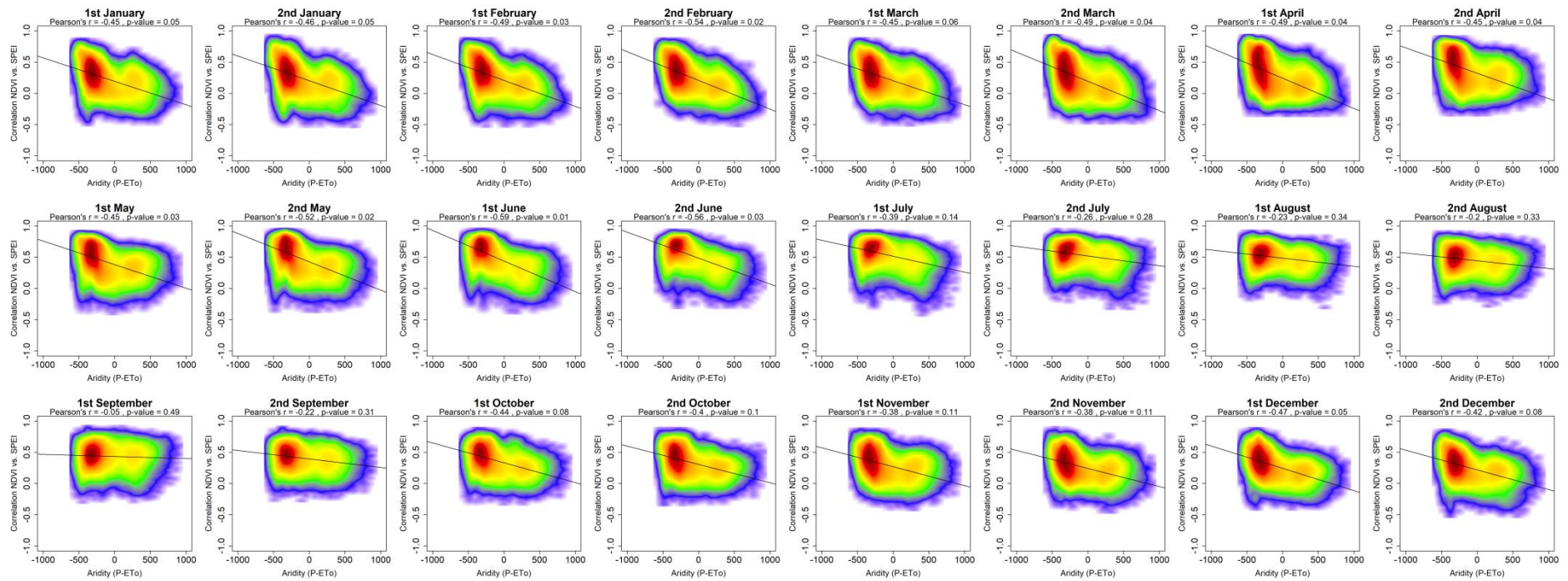
Figure 8. Scatterplots showing the relationships between the maximum correlation obtained between the sNDVI and the SPEI and the climate aridity (Precipitation minus ETo). Given the high number of data, the signification of the correlation was obtained by a bootstrap method. 1000 random samples were extracted of 30 data points each, from which correlations and p-values were obtained. The final signification was assessed by means of the average of the obtained correlation coefficients and p-values, which are indicated in the figure.
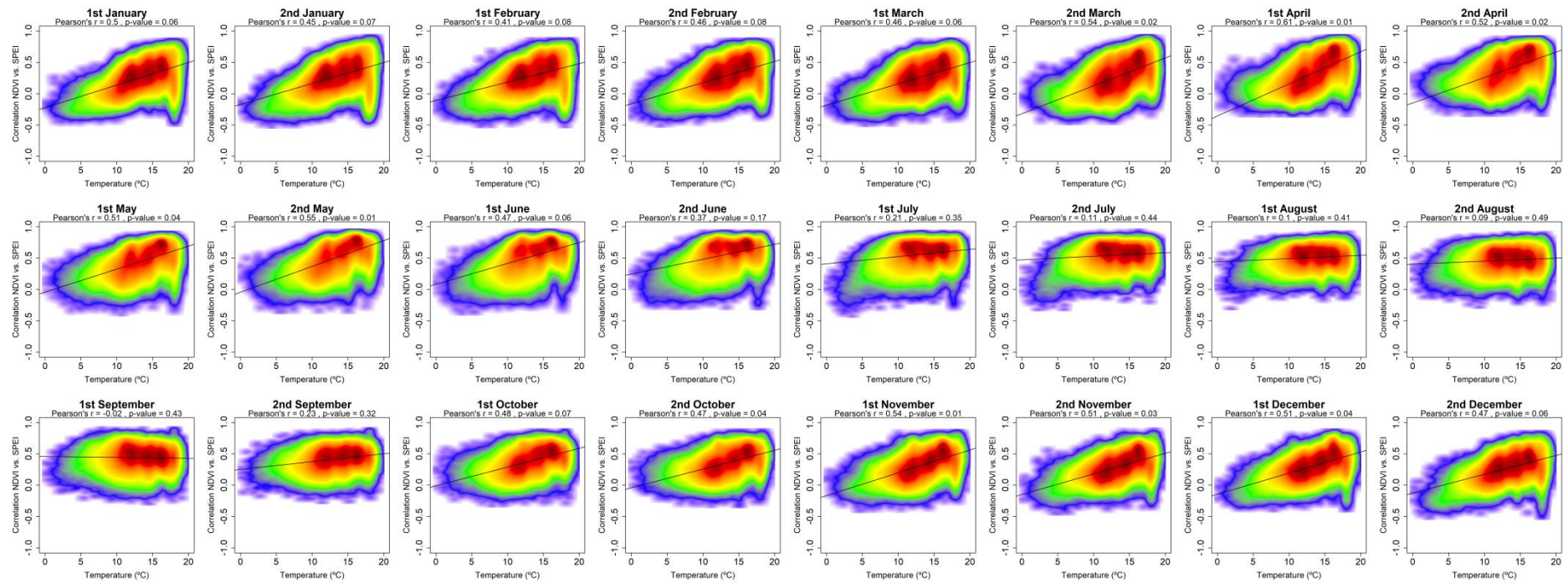
Figure 9. Scatterplots showing the relationships between the maximum correlation obtained between the sNDVI and the SPEI and the average air temperature. Given the high number of points the signification of correlation was obtained by means of 1000 random samples of 30 cases from which correlations and p-values were obtained. The final signification was assessed by means of the average of the obtained p-values.

Figure 10: Box plots showing the climate aridity values, as a function of the SPEI time scales at which the maximum correlation between the sNDVI and SPEI is recorded

Figure 11: Box plots showing air temperature values, as a function of the SPEI time scales at which the maximum correlation between the sNDVI and SPEI is recorded.
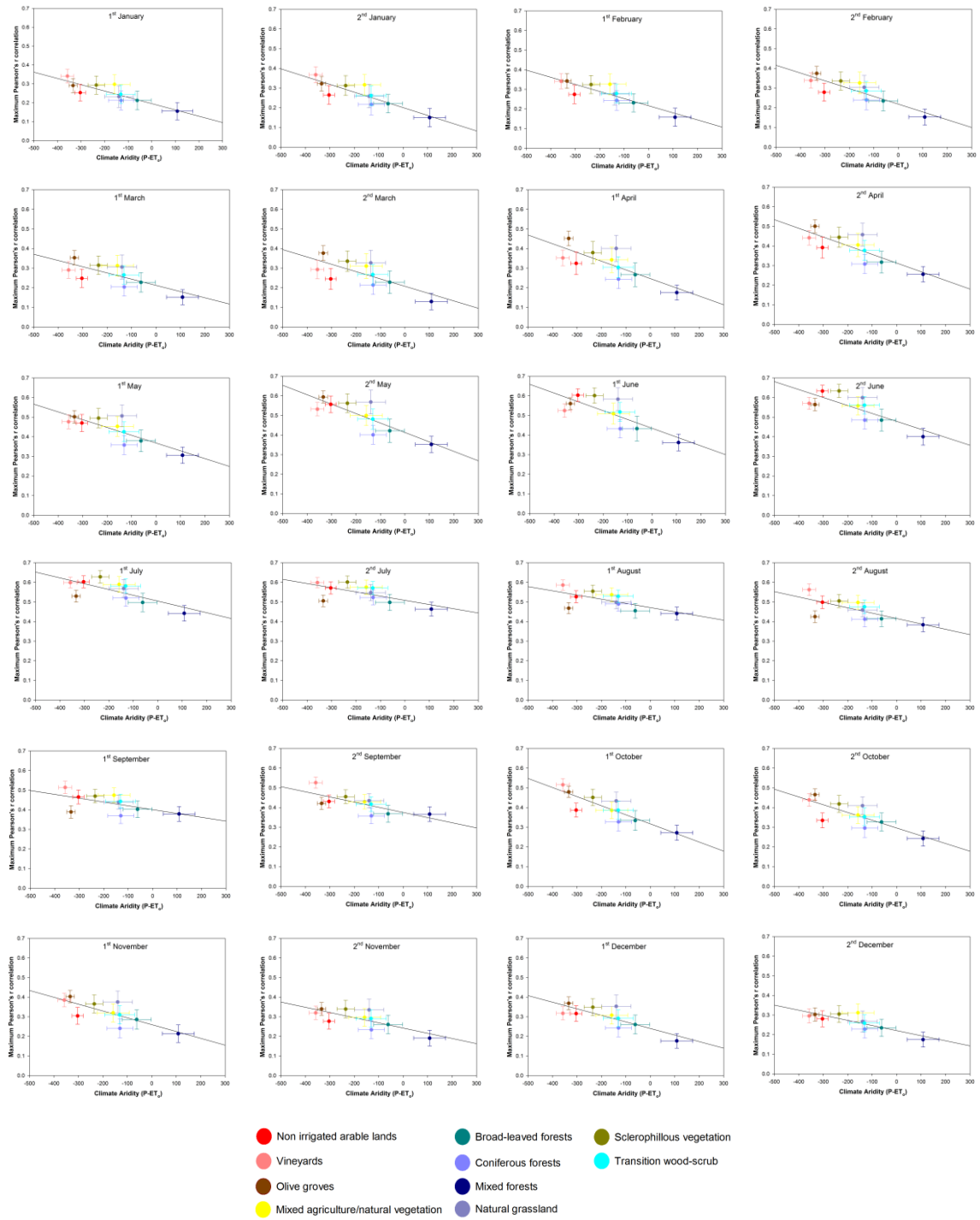
Figure 12: Scatterplots showing the relationship between the mean annual aridity and the maximum correlation found between the sNDVI and the SPEI in the different land cover types analysed in this study. Vertical and horizontal bars represent ¼ of standard deviation around the mean values.
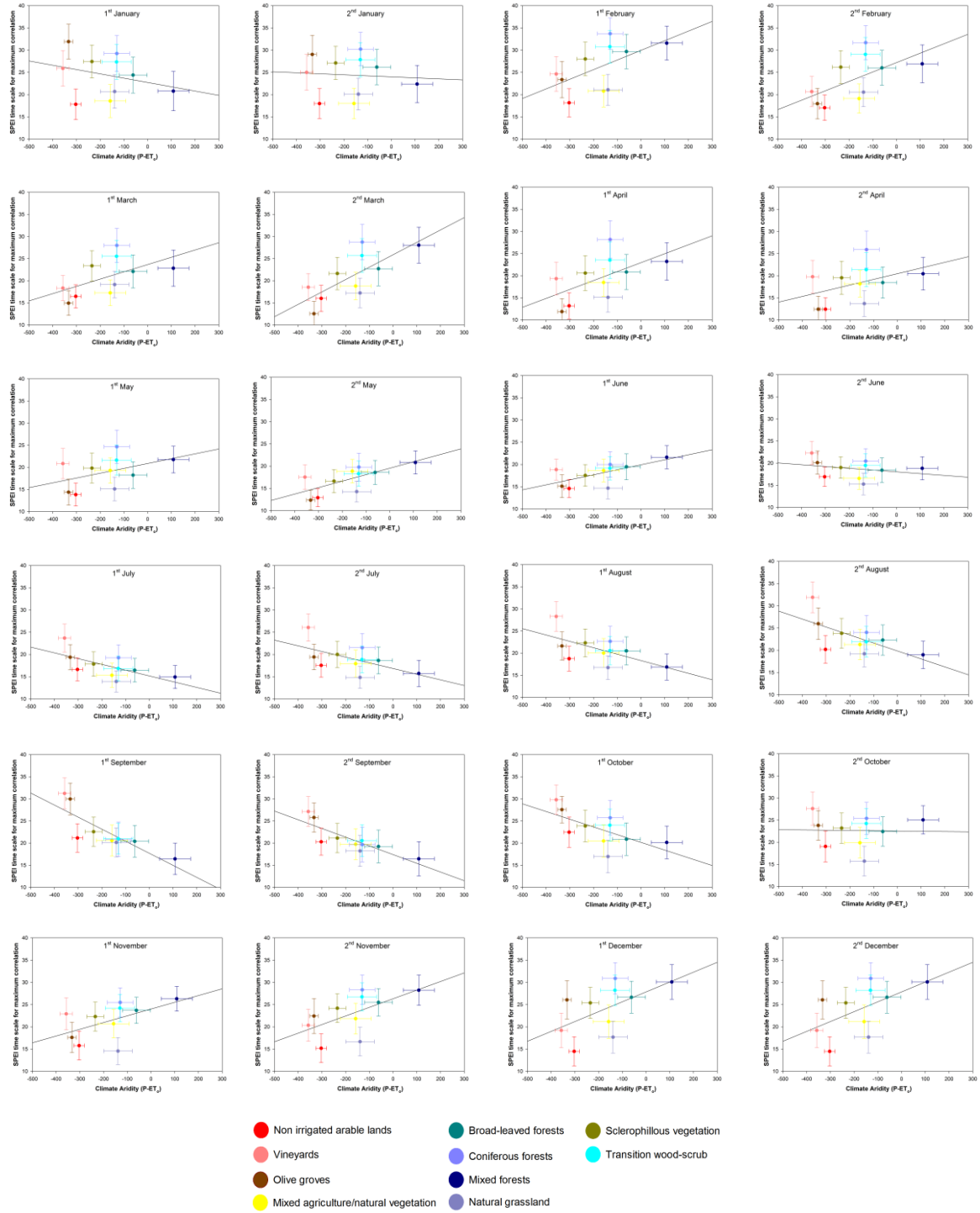
Figure 13: Scatterplots showing the relationship between the mean annual aridity and the SPEI time scale at which the maximum correlation is found between the sNDVI and SPEI for the different land cover types. Vertical and horizontal bars represent ¼ of standard deviation around the mean values.